



Silica Induction of Diverse Inflammatory Proteome in Lungs of Lupus-Prone Mice Quelled by Dietary Docosahexaenoic Acid Supplementation

Lichchavi D. Rajasinghe^{1,2†}, Melissa A. Bates^{1,2‡}, Abby D. Benninghoff³, Kathryn A. Wierenga⁴, Jack R. Harkema⁵ and James J. Pestka^{1,2,6*}

OPEN ACCESS

Edited by:

Reinaldo B. Oria,
Federal University of Ceara, Brazil

Reviewed by:

Kymerly Mae Gowdy,
The Ohio State University,
United States
Evelyn Tsantikos,
Monash University, Australia

*Correspondence:

James J. Pestka
pestka@msu.edu

†Present address:

Lichchavi D. Rajasinghe,
AstraZeneca, Gaithersburg, MD,
United States

‡These authors have contributed
equally to this work

Specialty section:

This article was submitted to
Nutritional Immunology,
a section of the journal
Frontiers in Immunology

Received: 22 September 2021

Accepted: 06 December 2021

Published: 21 January 2022

Citation:

Rajasinghe LD, Bates MA,
Benninghoff AD, Wierenga KA,
Harkema JR and Pestka JJ
(2022) Silica Induction of Diverse
Inflammatory Proteome in Lungs of
Lupus-Prone Mice Quelled by Dietary
Docosahexaenoic Acid Supplementation.
Front. Immunol. 12:781446.
doi: 10.3389/fimmu.2021.781446

¹ Department of Food Science and Human Nutrition, Michigan State University, East Lansing, MI, United States, ² Institute for Integrative Toxicology, Michigan State University, East Lansing, MI, United States, ³ Department of Animal, Dairy and Veterinary Sciences, School of Veterinary Medicine, Utah State University, Logan, UT, United States, ⁴ Department of Biochemistry and Molecular Biology, Michigan State University, East Lansing, MI, United States, ⁵ Department of Pathobiology and Diagnostic Investigation, Michigan State University, East Lansing, MI, United States, ⁶ Department of Microbiology and Molecular Genetics, Michigan State University, East Lansing, MI, United States

Repeated short-term intranasal instillation of lupus-prone mice with crystalline silica (cSiO₂) induces inflammatory gene expression and ectopic lymphoid neogenesis in the lung, leading to early onset of systemic autoimmunity and rapid progression to glomerulonephritis. These responses are suppressed by dietary supplementation with the ω-3 polyunsaturated fatty acid docosahexaenoic acid (DHA). Here, we tested the hypothesis that dietary DHA supplementation suppresses cSiO₂-induced inflammatory proteins in bronchoalveolar alveolar lavage fluid (BALF) and plasma of lupus-prone mice. Archived tissue fluid samples were used from a prior investigation in which 6 wk-old lupus-prone female NZBWF1 mice were fed isocaloric diets containing 0 or 10 g/kg DHA for 2 wks and then intranasally instilled with 1 mg cSiO₂ or vehicle once weekly for 4 wks. Cohorts were terminated at 1, 5, 9 or 13 wk post-instillation (PI). BALF and plasma from each cohort were analyzed by high density multiplex array profiling of 200 inflammatory proteins. cSiO₂ time-dependently induced increases in the BALF protein signatures that were highly reflective of unresolved lung inflammation, although responses in the plasma were much less robust. Induced proteins in BALF included chemokines (e.g., MIP-2, MCP-5), enzymes (e.g., MMP-10, granzyme B), adhesion molecules (e.g., sE-selectin, sVCAM-1), co-stimulatory molecules (e.g., sCD40L, sCD48), TNF superfamily proteins (e.g., sTNFR1, sBAFF-R), growth factors (e.g., IGF-1, IGFBP-3), and signal transduction proteins (e.g., MFG-E8, FcγRIIB), many of which were blocked or delayed by DHA supplementation. The BALF inflammatory proteome correlated positively with prior measurements of gene expression, pulmonary ectopic lymphoid tissue neogenesis, and induction of autoantibodies in the lungs of the control and treatment groups. Ingenuity Pathway Analysis (IPA) revealed that IL-1β, TNF-α, and IL-6 were among the

top upstream regulators of the cSiO₂-induced protein response. Furthermore, DHA's effects were associated with downregulation of cSiO₂-induced pathways involving i) inhibition of ARE-mediated mRNA decay, ii) bacterial and viral pattern recognition receptor activation, or iii) TREM1, STAT3, NF- κ B, and VEGF signaling and with upregulation of PPAR, LXR/RXR and PPAR α /RXR α signaling. Altogether, these preclinical findings further support the contention that dietary DHA supplementation could be applicable as an intervention against inflammation-driven autoimmune triggering by cSiO₂ or potentially other environmental agents.

Keywords: systemic lupus erythematosus, chemokine, metalloproteinase, TNF superfamily, omega-3 fatty acid, autoimmunity, inflammation

INTRODUCTION

Systemic lupus erythematosus (lupus), a chronic autoimmune disease predominantly affecting young women of child-bearing age, is caused by the loss of immunological tolerance resulting from yet poorly understood interactions between an individual's genome and the environment (1, 2). Initial onset of this disease typically involves unresolved inflammation and incomplete clearance of dead cells, accumulation of self-antigens, and autoantibody production, leading to the formation of immune complexes. Tissue deposition of these complexes fosters cytokine and chemokine production, infiltration of mononuclear effector cells, and ultimately, cell death. Collectively, these pathologic effects promote systemic inflammation and tissue injury, adversely affecting multiple organs including kidney, skin, heart, lung, and brain (3). Frequent recurrent cycles of flaring and remission in lupus leads to permanent organ damage that, without treatment, can manifest as severe glomerulonephritis and end-stage renal disease (kidney failure). Lupus management includes therapies based on immunosuppression, lymphocyte depletion, and cytokine/chemokine neutralization with monoclonal antibodies or receptor antagonists (4). Limitations of existing treatments include heterogeneity of individual patient symptoms, diversity of responses to therapeutics, adverse side effects leading to permanent organ damage, and high expense leading to financial burden on the patient. Thus, there is clear need for alternative safe and low-cost interventions for lupus.

Environment can influence onset and progression of autoimmunity in individuals with a genetic predisposition towards lupus (5). Notably, crystalline silica dust (cSiO₂) exposure in construction, mining, and ceramics industries has been epidemiologically associated with lupus and other autoimmune diseases (6–9). Induction of autoimmunity can be recapitulated at the preclinical level by introduction of cSiO₂ dust particles into the lungs of mice predisposed to lupus (10–14). Our laboratory has found in lupus-prone female NZBWF1 hybrid mice that, following four repeated weekly intranasal instillations with cSiO₂, latency of glomerulonephritis onset is reduced by three months (15, 16). At the mechanistic level, airway instillation of cSiO₂ causes the persistent build-up of particle-bearing monocytes/macrophages, release of proinflammatory cytokines and chemokines, recruitment of

neutrophils and macrophages into the alveolar space, programmed and necrotic cell death, and accumulation of nuclear and cytoplasmic debris (17). These events facilitate perivascular accumulation of T-cells, B-cells, and IgG autoantibody-producing plasma cells, leading to formation of ectopic lymphoid tissues (ELT) in the lung. The centrality of the lung in cSiO₂-triggered lupus onset and progression in NZBWF1 mice provides a unique window into potential mechanisms for and interventions against autoimmune pathogenesis in humans exposed to this and other respirable particles in the environment.

Diet is another environmental factor that can influence onset and progression of autoimmunity, with lipids being of particular importance. Consumption of marine ω -3 polyunsaturated fatty acids (PUFAs) can ameliorate chronic inflammatory and autoimmune diseases (18) and extend human lifetime (19). Mechanisms underlying ω -3 attenuating effects include i) influencing membrane function by altering lipid rafts and signaling, ii) moderating gene expression by repressing/activating transcription factors, iii) competition with ω -6 PUFA for metabolic enzyme binding sites and iv) serving as substrates for formation of pro-resolving metabolites [reviewed in (18, 20, 21)]. Unfortunately, Western diets contain large amounts plant- and animal-derived fats, therefore skewing tissue phospholipid fatty acid content overwhelmingly towards the more proinflammatory ω -6 PUFAs and away from the anti-inflammatory ω -3 PUFAs (22, 23). However, this imbalance can be overcome by eating fish or dietary fish/microalgal oil supplements containing the ω -3 PUFAs docosahexaenoic acid (C22:6 ω -3; DHA) and eicosapentaenoic acid (C20:5 ω -3; EPA). Relevant to the present study, dietary supplementation with ω -3 PUFA-rich fish oil inhibits inflammatory gene expression, production of autoantibodies, glomerulonephritis, and/or death in numerous murine preclinical lupus models (24–29), with DHA-enriched fish oil being most efficacious (30, 31). Consistent with these mouse studies, several clinical investigations support the assertion that increased ω -3 PUFA consumption might benefit patients with lupus (21, 32–34).

To ascertain how ω -3 PUFAs influence environment-triggered lupus flaring, Bates and coworkers (16) compared cSiO₂-triggered autoimmune disease onset and progression in autoimmune-prone female NZBWF1 mice fed control diets or diets containing DHA at the realistic human caloric equivalent of 2 or 5 g/d. After 2 wk on these dietary regimens, mice were

treated weekly for 4 wk with intranasally instilled cSiO₂ (1 mg) and then sacrificed 1, 5, 9, and 13 wk. DHA supplementation dose-dependently reduced cSiO₂-triggered B- and T-cell, follicular dendritic cell, and IgG⁺ plasma cell accumulation in the lungs along with development of glomerulonephritis. Subsequently, tissues from the aforementioned study were analyzed for 800 immune-related genes using targeted multiplex platform (35). Intriguingly, pulmonary transcriptome signatures of cSiO₂-treated mice fed control diet were indicative of progressive increases of genes associated with inflammation, innate/adaptive immunity, chemokines, type 1 interferon (IFN) responses, and antigen processing. Remarkably, DHA supplementation dose-dependently attenuated these responses, suggesting that consumption of this fatty acid impedes gene responses that play a central role in inflammation, ectopic lymphoid tissue neogenesis, and autoimmunity.

It is not yet known how modulation of cSiO₂-induced gene expression by DHA influences the inflammatory proteome. We therefore conducted a targeted proteomic analysis of archived tissue fluids from the Bates et al. study (16) to test the hypothesis that short-term repeated pulmonary exposures of lupus-prone mice to cSiO₂ induces inflammatory proteins in alveolar fluid and plasma, which are suppressed by DHA consumption. The results establish that cSiO₂ elicited a diverse inflammatory proteome in the lung that was consistent with unresolved inflammation and pulmonary ectopic lymphoid neogenesis and, furthermore, dietary DHA supplementation markedly quelled this robust inflammatory protein response.

MATERIALS AND METHODS

Experimental Design

This study employed archived tissues from our prior investigation (16) that was approved by the Institutional Animal Care and Use Committee at Michigan State University (AUF #01/15-021-00). Briefly, as depicted in **Figure 1A**, 6-wk old female lupus-prone NZBWF1 mice (Jackson Laboratories, Bar Harbor, ME) were fed control (CON) diet containing 10 g/kg corn oil and 60 g/kg high-oleic safflower oil (Hain Pure Food, Boulder, CO), whereas the intervention diet (DHA) included 10 g/kg corn oil, 35 g/kg high-oleic safflower oil and 25 g/kg microalgal oil containing 40% DHA (DHASCO, DSM Nutritional Products, Columbia MD). Resulting diets had 0 or 10 g/kg DHA, respectively, which were calorically equivalent to human doses of 0 and 5 g per day, respectively. After 2 wk maintenance on designated diets, mice were anesthetized with 4% isoflurane and instilled intranasally with 1.0 mg cSiO₂ (1.5–2.0 μm average particle size, U.S. Silica, Berkeley Springs, WV) in 25 μl PBS or 25 μl PBS vehicle (VEH) alone. Afterwards, mice were fed assigned diets for the experiment duration. Cohorts (n=8/group) were terminated at 1, 5, 9, and 13 wk post-instillation (PI) of the final cSiO₂ dose and bronchoalveolar lavage fluid (BALF), blood, and organs were collected, processed, and stored at -80°C as described previously (16). These specified times correspond with cSiO₂-induced histopathologic, transcriptomic, and autoimmune effects in NZBWF1 mice (16, 35, 36).

Targeted Inflammatory Proteomic Analysis by High Density Microarray ELISA

Selected samples (n=5/group) of BALF from 1, 5, 9, and 13 wk PI and plasma from 5, 9, and 13 wk PI were analyzed by RayBiotech (Norcross, GA) for the expression of 200 immune-related proteins using the Quantibody Array Q4000 (catalog #QAM-CAA-4000). Inflammation-associated proteins on the array were identified and functionally classified by RayBiotech as: i) chemokines, ii) adhesion molecules, iii) co-stimulatory molecules, iv) enzymes, v) signal transduction proteins, vi) TNF superfamily, vii) growth factors, and viii) cytokines (**Supplementary Table 1**). Briefly, BALF and plasma were diluted 3-fold and incubated for 2 h on glass arrays containing immobilized analyte-specific capture antibodies. Following incubation and washing, a cocktail of analyte-specific biotinylated detection antibodies was added and incubated for 2 h. After washing, arrays were incubated with Cy3-labeled streptavidin. A GenePix 4000B Microarray Scanner (Molecular Devices, Sunnyvale, CA) was used for fluorescent image acquisition. Resultant images were then digitized using GenePix software (Molecular Devices). Fluorescent intensities were acquired in quadruplicate for each sample and readings averaged to obtain mean fluorescent intensity (MFI). Signal to noise ratios (SNRs) were determined by comparing MFI to background signal for a specified analyte. SNRs greater than 2.0 were deemed positive for analyte signal above background.

Data Analysis

Heat mapping with unsupervised hierarchical clustering (HCC) and Principal Component Analysis (PCA) were visualized using ClustVis (37). For heat mapping, normalized and unit variance-scaled Z-scores were depicted.

$$Z = (x - \text{mean}) / \text{stdev}.$$

Values were centered by rows with imputation used for missing value estimation and rows were clustered using Euclidean distance and Ward linkage. Initial statistical analyses included pairwise Student's *t*-tests for all proteins to determine difference in expression for cSiO₂-exposed mice provided CON or DHA diet to the vehicle control (VEH/CON). Following this exploratory analysis, select proteins were further examined by scatter plot (Prism v. 8.3.0, GraphPad, San Diego, CA). The robust regression and outlier removal (ROUT) method was employed to discern outliers, which were excluded from further analysis (Q = 0.5%). Data were analyzed by two-way ANOVA for experimental factors time point and treatment and their interaction, with *post-hoc* Tukey HSD multiple comparisons test to determine the effect of treatment at each time point. If individual groups failed to pass at least one normality for Gaussian distributions tests (Shapiro-Wilk, Kolmogorov-Smirnov, Anderson-Darling, D'Agostino-Pearson omnibus), data were log-transformed.

Spearman rank correlation analyses were performed using *cor* and *corrplot* functions in R (www.R-project.org) or using Prism (GraphPad). A significant correlation was inferred when $\rho > 0.5$ or $\rho < -0.5$ and $p < 0.05$. To corroborate protein expression data, Spearman rank correlations were performed between protein expression data from this study and gene expression data previously reported for

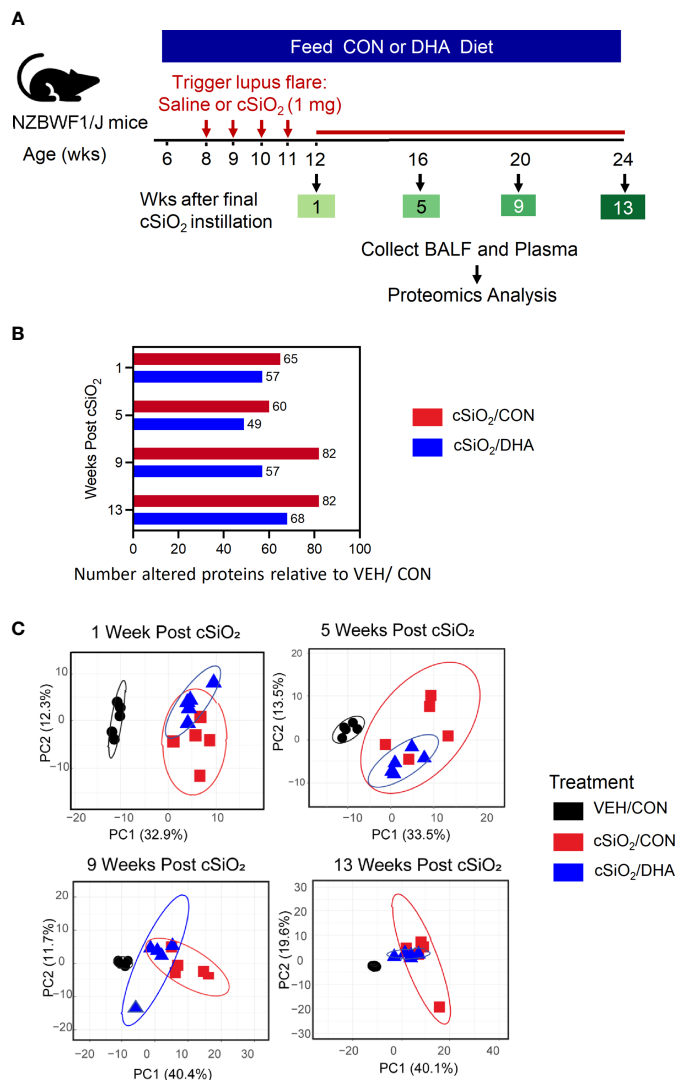


FIGURE 1 | Experimental design and inflammatory protein analysis of BALF. **(A)** Feeding of control (CON) or DHA diets was initiated in 6 wk-old female NZBWF1 mice. Two wk later, groups were intranasally instilled with 1 mg cSiO₂ or vehicle weekly for 4 wk. Animals were sacrificed at 12, 16, 20, or 24 wk of age, corresponding to 1, 5, 9, or 13 wk post final instillation (PI), respectively. Plasma and BALF were collected and analyzed for inflammatory proteins by high throughput multiplexed array. **(B)** cSiO₂ induced fewer proteins in BALF of mice fed DHA diet over time than those fed control diet. **(C)** PCA of differentially expressed protein in BALF of VEH/CON, cSiO₂/CON and cSiO₂/DHA over time. Ellipses indicate 95% confidence intervals.

corresponding animals (35), with both data sets represented as log₂ fold-change in expression levels relative to the VEH/CON group. Log₂ fold-changes in protein expression (expressed as MFI) relative to the VEH/CON group were calculated and correlated to the corresponding gene expression values. Spearman rank correlations for gene-protein interactions were determined using Microsoft Excel and bar graphs generated using GraphPad Prism.

Spearman rank correlations were also used to relate protein expression Z-scores with histological endpoints that included CD45R⁺ (B cells), CD3⁺ (T cells), CD21/35⁺ (follicular dendritic cells), and lymphoid aggregates, expressed as percent of lung area analyzed, which are collectively indicative of ectopic lymphoid neogenesis (16). For correlations to autoantibody production,

signal intensities for individual autoantibodies (Ab-score) were used (36).

IPA Analysis

Protein interactions and functional networks in the data set were determined using Ingenuity Pathway Analysis (IPA, QIAGEN Inc., Redwood City, CA). Calculated log₂ fold-change protein values (sample MFI relative to mean MFI for VEH/CON group) for each protein were submitted for IPA core analysis with the protein's UniProt identifiers. Protein expression was compared against its corresponding gene/protein expression data in the Ingenuity Pathway Knowledge Base. Canonical pathways and upstream

regulator analysis tools in IPA core analysis were used at default setting to explore cSiO₂ triggered immune-related pathways and predict expression of upstream regulators. The results from canonical pathways and upstream regulators analysis for different treatments groups were compared using comparison tool in IPA and visualized with GraphPad Prism. Proteins in data set with Z-scores ≥ 2 or ≤ -2 with an overlapping p-value < 0.05 were considered to be significantly activated or significantly inhibited, respectively, for all analyses or predictions.

RESULTS

Induction of Diverse Inflammatory Proteome by cSiO₂ in BALF Was Influenced by DHA Supplementation

Repeated intranasal instillations of cSiO₂ in CON-fed lupus-prone NZBWF1 induced increased expression of a diverse group of proteins in BALF relative to baseline over time that were highly reflective of unresolved inflammation in the lung, with significant elevations in 65, 60, 82, and 82 proteins being observed at 1, 5, 9, and 13 wk PI, respectively (**Figure 1B**). DHA feeding reduced the number of proteins elevated at each timepoint, with cSiO₂-treated DHA-fed mice exhibiting elevations in 57, 49, 57, and 68 proteins at 1, 5, 9, and 13 wk PI, respectively. PCA analysis further indicated that inflammatory proteomes in the BALF of cSiO₂/CON and cSiO₂/DHA mice at 1, 5, 9, and 13 wk PI were overlapping but different from those of VEH/CON mice (**Figure 1C**).

Heat mapping revealed that cSiO₂ treatment induced numerous chemokines (e.g., MIP-2, MCP-5), enzymes (e.g., MMP-10, granzyme B), adhesion molecules (e.g., E-selectin, VCAM-1), co-stimulatory molecules (e.g., CD40L, CD48), TNF superfamily proteins (e.g., TNFR1, BAFF-R), growth factors (e.g., IGF-1, IGFBP-3), and signal transduction proteins (e.g., MFG-E8, FcγRIIB) in the BALF (**Figure 2** and **Supplementary File 1**). Most of these were upregulated beginning at 5 wk PI and continued to increase over time, while time-matched VEH control groups remained unchanged or slightly increased. A small subset of cSiO₂-induced inflammatory proteins in CON-fed mice were modestly elevated at 9 wk PI and remained so at 13 wk PI. DHA supplementation suppressed or delayed release of many cSiO₂-induced proteins in BALF, particularly at 5 and 9 wk PI but less so at wk 13 suggesting some diminishment of DHA's ameliorative effects. Spontaneous production of some proteins was also observed at 5, 9 or 13 wk PI in VEH control groups compared to earlier time points. The influence of time and treatment on specific protein families is described in further detail and illustrated in heat maps below.

Chemokines Were Robustly Induced by cSiO₂ in BALF and Suppressed by DHA Feeding While Cytokines Were Minimally Affected

cSiO₂ elicited vigorous and diverse chemokine responses in BALF of CON-fed mice (**Figure 3A**). Effects were detected as early as 1 wk PI (MIP-2 and MIP-3b), whereas induction of

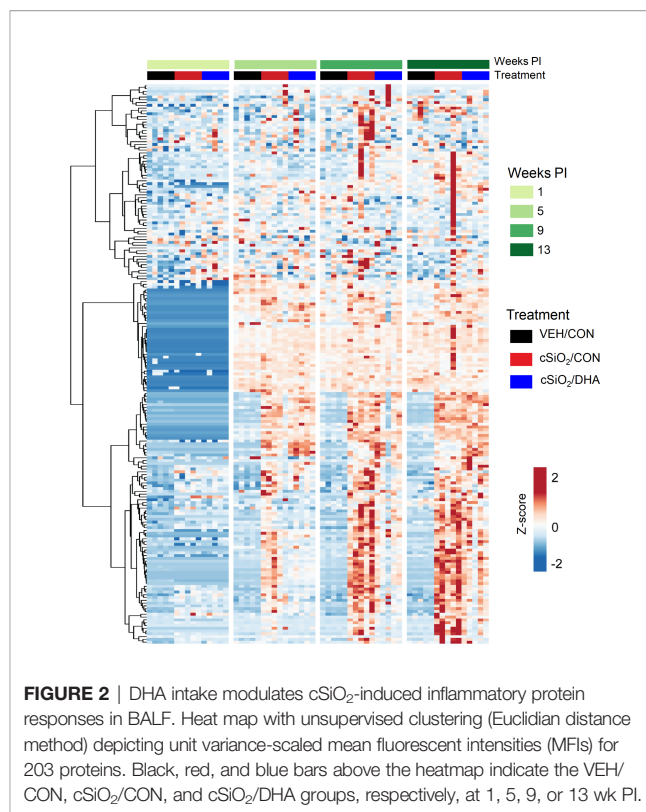


FIGURE 2 | DHA intake modulates cSiO₂-induced inflammatory protein responses in BALF. Heat map with unsupervised clustering (Euclidean distance method) depicting unit variance-scaled mean fluorescent intensities (MFIs) for 203 proteins. Black, red, and blue bars above the heatmap indicate the VEH/CON, cSiO₂/CON, and cSiO₂/DHA groups, respectively, at 1, 5, 9, or 13 wk PI.

others were not manifested until 5 wk PI (MIG, eotaxin-1) or 9 wk PI (MCP-5, RANTES, MIP-3a, I-TAC, BLC) (**Figure 3B**). DHA supplementation suppressed induction of these chemokines, particularly at wk 9 and 13 PI (**Figures 3A, B**). In contrast to robust chemokine responses, cSiO₂ instillation did not have a large effect on BALF cytokines, with only modest upregulation being observed for IL-1 α at 1 wk PI, IL-2Ra and IL-6 at 5 wk PI, and IL-17E and IL-17F at wk 9 PI (**Supplementary Figure 1**). Of these, only IL-2RA, IL-17E, and IL-17F induction were suppressed by DHA feeding.

cSiO₂-Triggered Elevations of Enzymes, Adhesion Molecules, and Co-Stimulatory Molecules in BALF Were Inhibited by DHA Feeding

cSiO₂ triggered expression of diverse enzymes in BALF including MMP-3, ACE, and Axl at wk 1 PI, granzyme B at 5 wk PI, and MMP-10 and renin at 9 wk PI (**Figures 4A, B**). These responses were inhibited or delayed in cSiO₂-treated DHA-fed mice. cSiO₂ exposure further induced early and marked release of soluble adhesion molecules into the BALF of CON-fed mice as demonstrated by elevated sE-selectin, sL-selectin, sP-cadherin, sVCAM-1, and periostin at 1 wk PI and P-selectin at 5 wk PI in the BALF (**Figures 5A, C**). Increased soluble costimulatory molecules were also evident in CON/cSiO₂ mice by 1 wk PI (CD40L, CD48) or 9 wk PI (CD6) (**Figures 5B, D**). While relative MFIs of these soluble adhesion and costimulatory molecules rose over time, these progressive

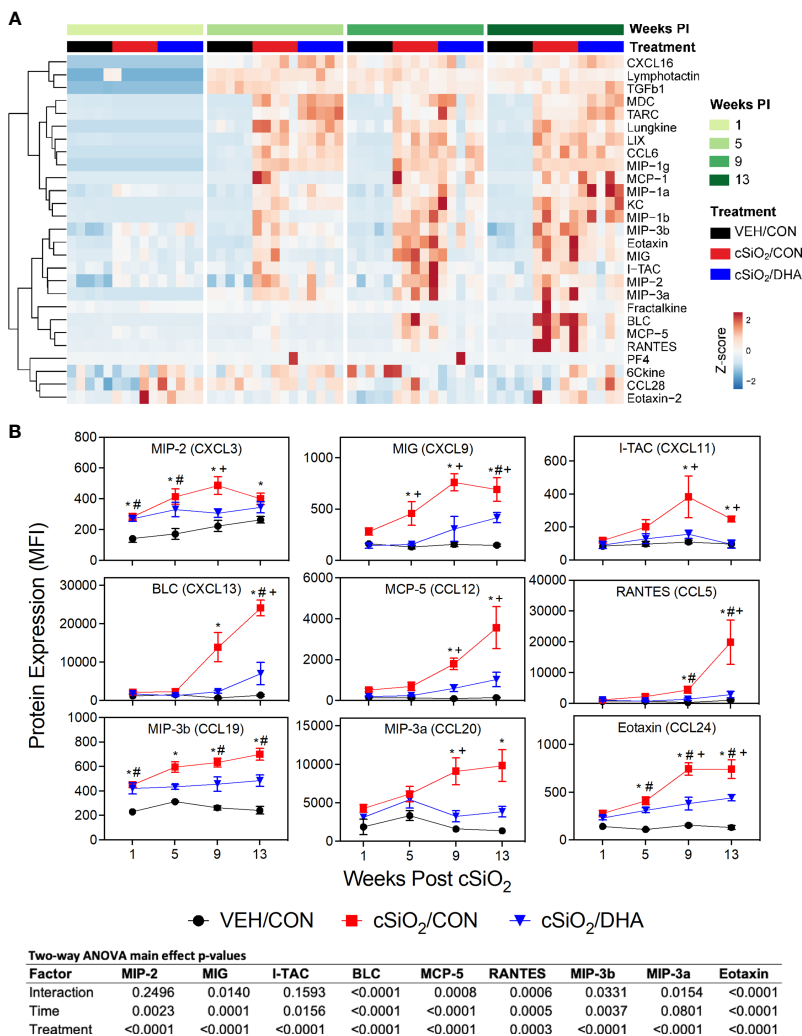


FIGURE 3 | Consumption of DHA suppresses cSiO₂-triggered chemokine expression in BALF. **(A)** Heat maps with unsupervised clustering (Euclidian distance method) depict unit variance-scaled mean fluorescent intensities (MFIs) for chemokine expression measured in the BALF. Black, red, and blue bars above the heatmap indicate the VEH/CON, cSiO₂/CON, and cSiO₂/DHA groups, respectively, at 1, 5, 9, or 13 wk PI. Scale bar values reflect the range of variance-stabilized MFIs, which were centered across rows. **(B)** DHA feeding suppressed selected cSiO₂-induced chemokines in BALF over time. MFIs were obtained using the microarray panel for VEH- or cSiO₂-exposed mice fed CON or DHA diet. Data for select proteins were analyzed by two-way ANOVA for main effects of timepoint and treatment with *post-hoc* Tukey HSD multiple comparison tests to determine effects of treatment at each time point. Data are mean ± SEM. Main effect p-values for timepoint, treatment, and the interaction of these factors are shown below the plots. Symbols indicate significant differences ($p \leq 0.05$) as follows: * for cSiO₂/CON vs. VEH/CON; # for cSiO₂/DHA vs. VEH/CON; and + for cSiO₂/CON vs. cSiO₂/DHA.

increases were significantly delayed by DHA supplementation (Figures 5B–D).

DHA Supplementation Slowed TNF Superfamily Elevation but Differentially Influenced Signal Transduction Molecule Release in BALF in Response to cSiO₂

Instilling the lungs of CON-fed mice with cSiO₂ also induced release of several soluble TNF superfamily members into BALF that were evident as early as 1 wk PI (TNFR1, TNFR2, and CD40) or later at 9 wk PI (BAFF-R, OX40L, and TRAIL) (Supplementary Figure 2). TNF superfamily responses were

markedly delayed by feeding DHA. cSiO₂ also elicited increases in soluble signal transduction molecules in BALF that included MFG-E8, FcγRIIB, and galectin-1 at 1 wk PI, leptin and MBL-2 at 5 wk PI, and resistin and B7-1 at 9 wk PI (Supplementary Figure 3). While DHA supplementation delayed leptin, FcγRIIB, galectin-1, and B7-1 responses, it enhanced MFG-E8 release.

Rapid Induction of Diverse Growth Factor Proteins by cSiO₂ Was Suppressed by DHA Consumption

cSiO₂ instillation triggered elevations in IGF-1, IGFBP-3, decorin, epiregulin, Gas-1, fetuin A, PIGF-2 by 1 or 5 wk PI,

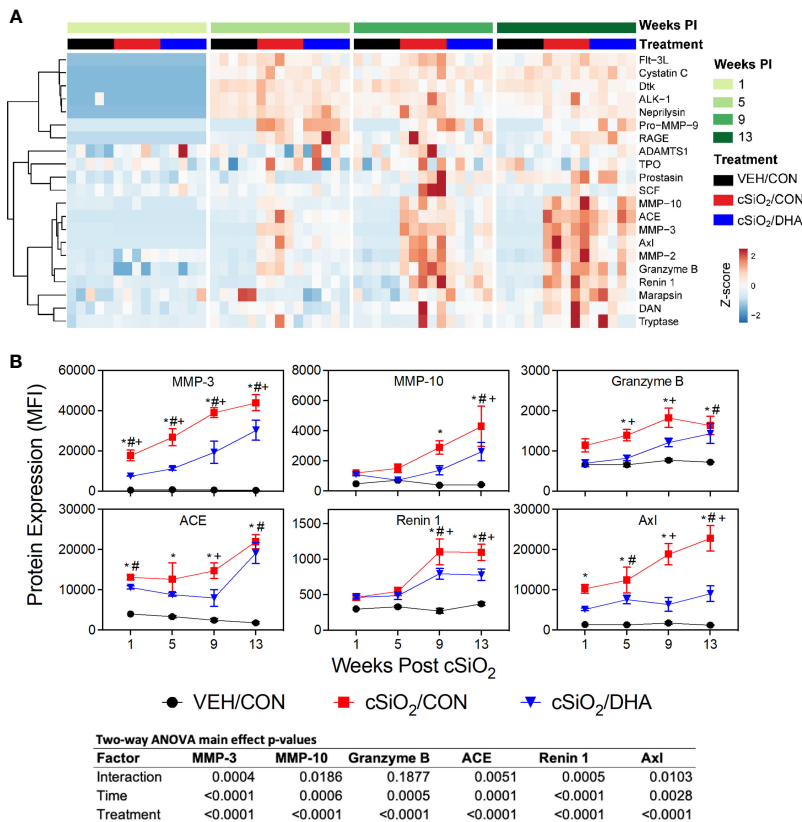


FIGURE 4 | DHA supplementation inhibits cSiO₂-stimulated release of inflammation-associated enzymes into the BALF. **(A)** Heat map with unsupervised clustering (Euclidian distance method) depicts unit variance-scaled mean fluorescent intensities (MFIs) for enzyme expression measured in the BALF. Black, red and blue bars above the heat map indicate the VEH/CON, cSiO₂/CON, and cSiO₂/DHA groups, respectively, at 1, 5, 9, or 13 wk PI. Scale bar values reflect the range of variance-stabilized MFIs, which were centered across rows. **(B)** DHA diet suppresses cSiO₂ induction of selected enzymes in BALF over time. MFIs were obtained using the microarray panel for VEH- or cSiO₂-exposed mice fed CON or DHA diets. Data for select proteins were analyzed by two-way ANOVA for main effects of timepoint and treatment with *post-hoc* Tukey HSD multiple comparison tests to determine effects of treatment at each time point. Data are mean ± SEM. Main effect p-values for timepoint, treatment, and the interaction of these factors are shown below the plots. Symbols indicate significant differences ($p \leq 0.05$) as follows: * for cSiO₂/CON vs. VEH/CON; # for cSiO₂/DHA vs. VEH/CON; and + for cSiO₂/CON vs. cSiO₂/DHA.

and, additionally, progranulin and G-CSF by wk 9 PI in CON-fed mice, whereas all but one of the growth factor responses were markedly suppressed in DHA-fed mice (Figures 6A, B).

BALF Protein Responses Correlate Positively With Gene Expression and Autoimmune Pathogenesis in the Lung

Where data sets overlapped, expression of proteins in the BALF correlated positively with the genes that encode them, as determined by mRNA expression of lung-associated genes assessed in our previous study (35) (Figure 7). These associations were strongest at 9 wk PI but also observed at 5 and 13 wk PI, albeit to a lesser extent. Specific proteins included chemokines (CCL6, CXCL16, eotaxin-1, I-TAC, KC, LIX, lungkine, MCP-1, MCP-5), cytokines (GM-CSF, IL-10, IL-12p40, IL-17F, IL-1a, IL-1ra, IL-2 Ra, IL-21, IL-28, IL-6), enzymes (Axl, granzyme B, Pro-MMP-9), adhesion molecules (E-selectin, VCAM-1, Icam1), co-stimulatory molecules (CD48, CD6, CTLA4), TNF superfamily proteins (BAFFR, Fas, GITR, TNFRI, TNF α , TRAIL, TRANCE, TWEAK, 4-1BB), and signal transduction

proteins (clusterin, CRP, Fc γ RIIB, lipocalin-2, MBL-2, TREM1). Thus, mRNA expression in the lung was reasonably predictive of inflammatory proteins in the alveolar fluid.

BALF protein responses for individual mice strongly correlated with histopathologic scoring of ELT development and with quantitative morphometry of CD45R⁺ B-cells, CD3⁺ T-cells, and CD21/35⁺ follicular dendritic cells in lungs of cSiO₂-exposed mice, with strongest associations being observed at 13 wk PI (Figure 8A). Moreover, protein responses in individual mice correlated positively with IgG autoantibodies associated with Sm antigens, DNA related nucleoproteins, DNA organization and nuclear membrane proteins, La/SBB antigens, Ro/SSA antigens, RNA antigens, and phospholipids at 5, 9, and 13 wk PI (Figure 8B).

DHA Supplementation Interferes With Regulatory Pathways for cSiO₂-Triggered Inflammatory Protein Expression

Protein expression data were subjected to IPA to identify key upstream molecules regulating the inflammatory response of the

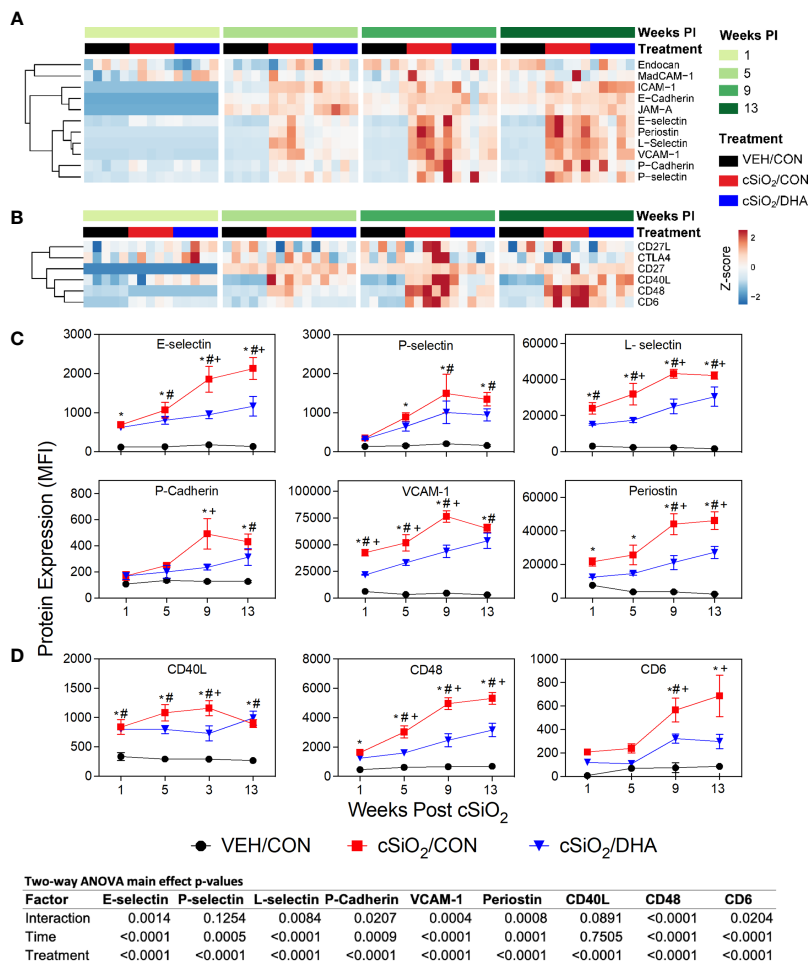


FIGURE 5 | DHA consumption suppresses cSiO₂-induced adhesion and co-stimulatory molecule release into the BALF. Heat maps with unsupervised clustering (Euclidian distance method) depict unit variance-scaled mean fluorescent intensities (MFIs) for **(A)** adhesion and **(B)** co-stimulatory molecules expression measured in the BALF. Black, red and blue bars above the heat map indicates the VEH/CON, cSiO₂/CON, and cSiO₂/DHA groups, respectively, at 1, 5, 9, or 13 wk PI. Scale bar values reflect the range of variance-stabilized MFIs, which were centered across rows. **(C, D)** Effects of DHA induction of selected **(C)** adhesion and **(D)** co-stimulatory molecules by cSiO₂ in BALF over time. MFIs were obtained using the microarray panel for VEH- or cSiO₂-exposed mice fed CON or DHA diets. Data for select proteins were analyzed by two-way ANOVA for main effects of timepoint and treatment with *post-hoc* Tukey HSD multiple comparison tests to determine effects of treatment at each time point. Data are mean ± SEM. Main effect p-values for timepoint, treatment, and the interaction of these factors are shown below the plots. Symbols indicate significant differences ($p \leq 0.05$) as follows: * for cSiO₂/CON vs. VEH/CON; # for cSiO₂/DHA vs. VEH/CON; and + for cSiO₂/CON vs. cSiO₂/DHA.

lung following cSiO₂ and DHA treatment. Based on activation Z-scores, IL-1 β , TNF- α , INF γ , IL-6, IL-17A, IL-4, and NF- κ B complexes were the top upstream inflammatory proteome regulators predicted to be activated following cSiO₂ instillation, whereas IL-10 was predicted to be inhibited following treatment with cSiO₂ (Figure 9A). Importantly, feeding DHA reduced activation Z-scores associated with cSiO₂-induced TNF- α , IL-1 β , INF γ , IL-17A, IL-4, IL-10 and NF- κ B complex, while increasing the inhibition Z-score for IL-10 (Figure 9A). Figures 9B, C reflect diverse cSiO₂-induced inflammatory proteome predicted to be downstream of IL-1 β and TNF- α , respectively.

IPA was further utilized to identify functionally linked pathways that were significantly influenced by cSiO₂ and DHA (Figure 10). DHA's effects were associated with downregulation of cSiO₂-induced pathways involving ARE-mediated mRNA

decay, TREM1 signaling, STAT3, NF- κ B signaling, bacterial and viral pattern recognition receptor activation, and VEGF signaling (Figure 10A) and upregulation of PPAR signaling, LXR/RXR activation, and PPAR α /RXR α activation (Figure 10B).

cSiO₂ and DHA Had Limited Effects on the Inflammatory Proteome in Plasma

In contrast to BALF, cSiO₂ and DHA had relatively modest effects on expression of most plasma proteins in the targeted array (Supplementary Figure 4 and Supplementary File 1). cSiO₂-treated CON-fed mice showed increases in 9, 7, and 15 proteins at 5, 9, and 13 wk PI, respectively. DHA again reduced expression of cSiO₂-induced proteins, as cSiO₂-treated DHA-fed mice showed elevations in 0, 1, and 2 proteins at 5, 9, and 13 wk PI, respectively (Supplementary Figure 5A). The chemokines

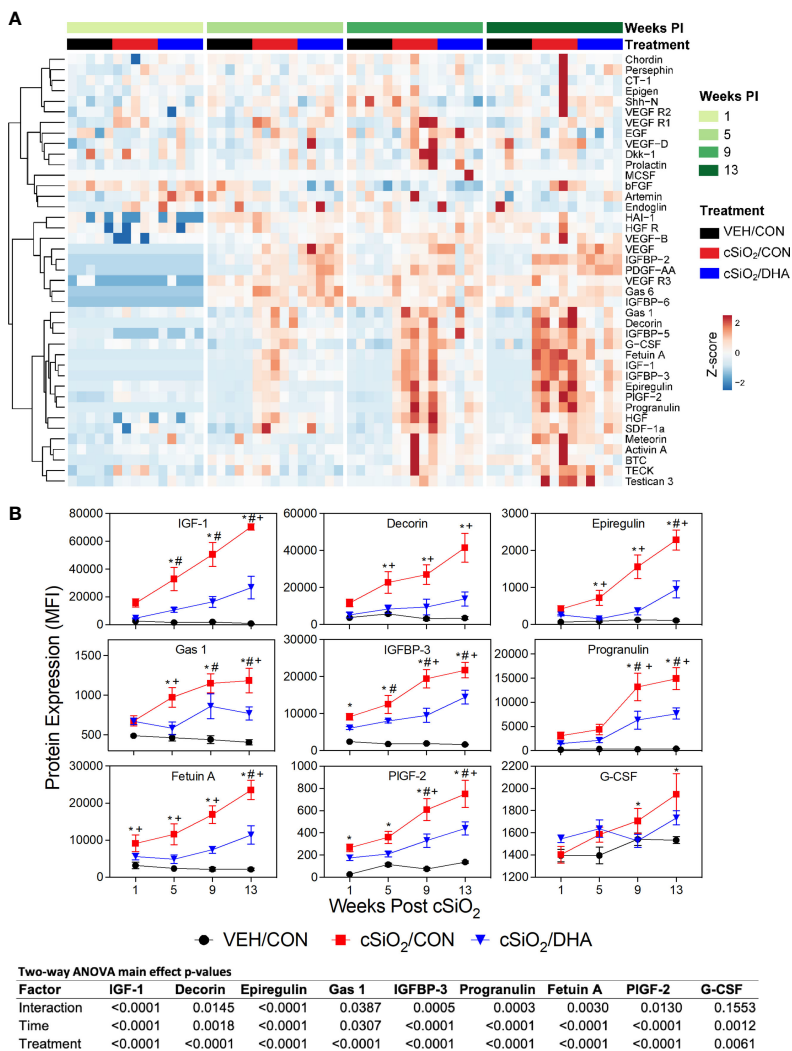


FIGURE 6 | cSiO₂-induced growth factor expression in BALF suppressed by intake of DHA diet. **(A)** Heat maps with unsupervised clustering (Euclidian distance method) depict unit variance-scaled mean fluorescent intensities (MFIs) for growth factor expression measured in the BALF. Black, red and blue bars above heat maps indicate the VEH/CON, cSiO₂/CON, and cSiO₂/DHA groups, respectively, at 1, 5, 9, or 13 wk PI. Scale bar values reflect the range of variance-stabilized MFIs, which were centered across rows. **(B)** Effect of DHA diet on cSiO₂ induction of selected growth factors in BALF over time. MFIs were obtained using the microarray panel for VEH- or cSiO₂-exposed mice fed CON or DHA diets. Data for select proteins were analyzed by two-way ANOVA for main effects of timepoint and treatment with *post-hoc* Tukey HSD multiple comparison tests to determine effects of treatment at each time point. Data are mean ± SEM. Main effect p-values for timepoint, treatment, and the interaction of these factors are shown below the plots. Symbols indicate significant differences (*p* ≤ 0.05) as follows: * for cSiO₂/CON vs. VEH/CON; # for cSiO₂/DHA vs. VEH/CON; and + for cSiO₂/CON vs. cSiO₂/DHA.

were the one functional group affected by the treatments. As illustrated in mean Z-score plots, chemokines were upregulated in plasma in CON-fed mice following cSiO₂ exposure mirroring effects seen in BALF (Supplementary Figures 5B, C). This upregulation was markedly suppressed in DHA-fed mice. Furthermore, chemokine protein responses in BALF in individual mice over the four time points modestly correlated with plasma chemokine protein responses (Supplementary Figure 5D). Notably, CCL6, I-TAC, BLC, and MCP-5 at 9 wk PI showed a strong positive correlation with plasma chemokines (Supplementary Figure 5E). Altogether, inflammatory protein responses to cSiO₂ and DHA were much more robust in the

pulmonary region than the systemic compartment, suggesting that the lung was the primary nexus for inflammation and autoimmunity in this model.

DISCUSSION

Since inhaled cSiO₂ particles are cleared slowly from the lung, they persist and drive a cycle in alveolar macrophages involving phagocytosis, phagolysosome permeabilization, and inflammasome activation that culminates in cell death and reentry of cSiO₂ into

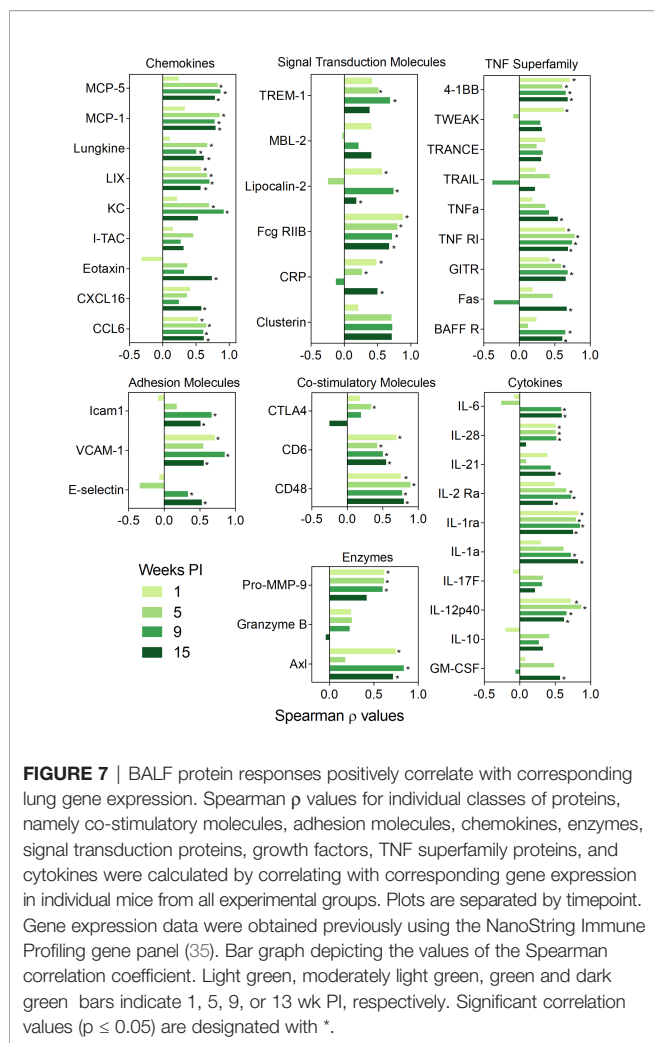


FIGURE 7 | BALF protein responses positively correlate with corresponding lung gene expression. Spearman ρ values for individual classes of proteins, namely co-stimulatory molecules, adhesion molecules, chemokines, enzymes, signal transduction proteins, growth factors, TNF superfamily proteins, and cytokines were calculated by correlating with corresponding gene expression in individual mice from all experimental groups. Plots are separated by timepoint. Gene expression data were obtained previously using the NanoString Immune Profiling gene panel (35). Bar graph depicting the values of the Spearman correlation coefficient. Light green, moderately light green, green and dark green bars indicate 1, 5, 9, or 13 wk PI, respectively. Significant correlation values ($p \leq 0.05$) are designated with *.

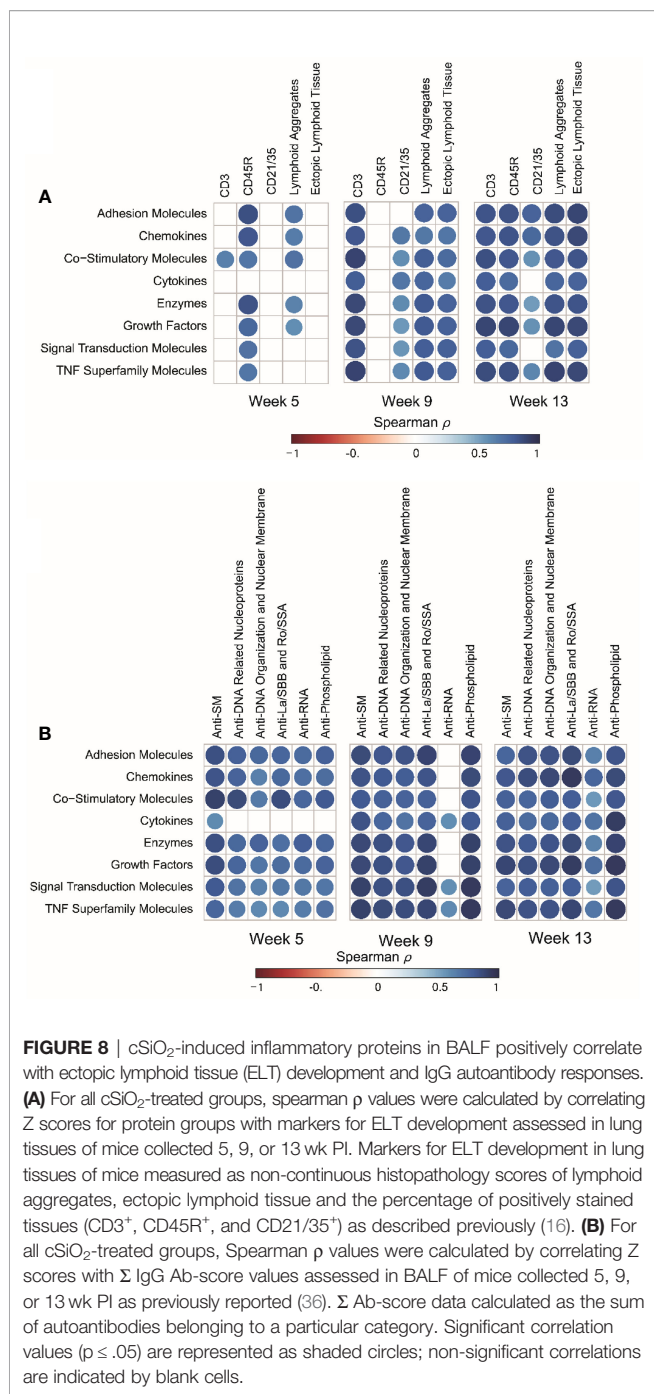
the alveolar space (17). Repetition of this cycle evokes chronic unresolved inflammation in the lung and release of self-antigens, leading to eventual loss of immune tolerance (38, 39). In prior studies with lupus-prone NZBWF1 female mice, we discovered that DHA feeding prior to cSiO₂ instillation suppresses progressive increases over wks 1, 5, 9, and 13 PI in inflammatory/autoimmune gene expression, inflammatory cell recruitment, and autoantibody production (16, 35, 36). For example, in mice fed a control diet without DHA, cSiO₂ instillation triggered a mixed inflammatory cell infiltrate in the lung (alveolitis composed of monocytes/macrophages, neutrophils and lymphocytes) with semiquantitative histopathology severity scores of minimal (1 out of 4) and mild to moderate (2/3 out of 4) at 1/5 and 9/13 wk PI, respectively (16). Likewise, total inflammatory cells in BALF from these cSiO₂-instilled mice were modestly increased at 1 and 5 wk PI and dramatically increased by 9 and 13 wk PI, as compared to saline vehicle-instilled animals fed the control diet. In contrast, cSiO₂ mice fed DHA supplemented diet (human daily equivalent 5 g/day) had minimal alveolitis at 1, 5, and 9 wk PI and only mild alveolitis at 13 wk PI. Total inflammatory cell

numbers in BALF of these DHA-supplemented mice were similarly suppressed at 9 and 13 wk PI (16).

The findings presented herein show for the first time how cSiO₂ and DHA influence the inflammatory proteome in BALF and plasma in this preclinical model of environment-triggered autoimmunity. First, cSiO₂ induced a diverse inflammatory proteome in the BALF that persisted and progressed long after particle exposure was ceased. Upregulated proteins included chemokines, enzymes, adhesion molecules, co-stimulatory molecules, growth factors, TNF superfamily members, and signal transduction proteins. Second, the plasma inflammatory protein responses to cSiO₂ were limited to chemokines and much less robust than observed in the BALF, confirming the lung to be the central site for inflammation and autoimmunity in this model. Third, DHA consumption markedly suppressed cSiO₂-induced expression of many of these inflammatory proteins in BALF at wks 1, 5, and 9 PI and, furthermore, DHA's ameliorative actions against some inflammatory proteins appeared to be lost at 13 wk PI. Fourth, correlation analyses confirmed that DHA's inhibitory effects on cSiO₂-induced inflammatory protein signatures corresponded with prior measurements of transcriptional responses, ectopic lymphoid structure development, and autoantibody production. Finally, DHA's ameliorative effects were associated with inhibition of proinflammatory cytokine-driven innate immune pathways and activation of lipid-signaling signaling pathways. Altogether, these new findings support the contention that DHA supplementation might be a promising intervention against cSiO₂-induced inflammation and autoimmune disease onset and flaring in susceptible individuals.

IPA analysis indicated that IL-1, IL-6, and TNF- α were among the chief regulators for predicted pathways mediating cSiO₂-triggered inflammatory proteins and that these pathways were downregulated by DHA. cSiO₂ instillation into the lung is well-known to acutely elicit secretion of proinflammatory cytokines such as IL-1 β , IL-1 α , IL-6, and TNF- α by direct or indirect action on alveolar macrophages, neutrophils, and epithelial cells (40–43). Therefore, it was surprising that cSiO₂'s effects on these proinflammatory cytokines in BALF were modest across the time cohorts of this study. Nevertheless, these low responses concurred with low expression of corresponding cytokine mRNAs in the parent study (35). The lack of a robust proinflammatory cytokine responses to prolonged cSiO₂ exposure compared to that for chemokines and other proteins likely reflects the strict regulation and relatively short half-lives of proinflammatory cytokine mRNAs and proteins in tissues due to their injurious potential (44).

Pathway analysis further revealed that DHA's quelling effects were associated with attenuation of ARE-mediated mRNA decay, TREM1, NF- κ B, and STAT3 signaling pathways, and potentiation of PPAR signaling and PPAR α /RXR α and LXR/RXR activation. In the parent investigation from which tissue fluids were sourced, we reported that total ω -3 PUFA and ω -6 PUFA represented 6.6 and 33.4% of lung lipids in cSiO₂-treated CON-fed mice, respectively, whereas in the cSiO₂-treated DHA-fed group, they were 23.2 and 16.3%, respectively (16). At the mechanistic level,



increasing the ω -3: ω -6 PUFA ratio might hamper lipid raft development and prevent activation of transmembrane receptors that control innate and adaptive immune processes (45). Additionally, DHA and EPA can be liberated from the membrane by intracellular and extracellular phospholipases (46, 47), allowing them to act as ligands for extracellular and intracellular receptors that inhibit proinflammatory signaling pathways (48, 49). Consistent with our IPA pathway analysis here, these receptors include PPAR and RXR family members that

downregulate NF- κ B- and STAT-dependent transcription of innate immune genes (50, 51). Moreover, DHA and EPA can directly compete with ω -6 PUFAs as enzymatic substrates for downstream bioactive lipid mediators, leading to reduced proinflammatory metabolites (e.g. prostaglandins, leukotrienes) and increased specialized pro-resolving metabolites (e.g. resolvins, protectins, maresins) that promote resolution of inflammation (52, 53). Accordingly, changing the tissue balance by enhancing ω -3 PUFAs and diminishing ω -6 PUFAs likely reduces the cSiO₂-induced inflammatory proteome by several independent or interdependent mechanisms.

The diverse array of inflammatory proteins induced by cSiO₂ in this lupus-prone mouse model provides new insights into how the particle triggers inflammation and autoimmunity and how such triggering might be ameliorated by consumption of DHA. Chemokines were foremost among the proteins induced by cSiO₂. The robust increases in BLC (B-lymphocyte chemoattractant; CXCL13) are particularly pertinent in ELT neogenesis. BLC, which is produced by follicular dendritic cells, T follicular helper cells, and Th17 cells, is essential for B-cell localization into lymphoid follicles. Other CXCL chemokines might also impact cSiO₂-induced autoimmunity. MIP-2 (CXCL3) primarily recruits neutrophils to sites of inflammation that, upon degranulation, could secrete proteolytic enzymes that elicit bystander tissue injury and inflammation, or release neutrophil extracellular DNA traps *via* NETosis, a source of self-DNA and autoantigens (54). Consistent with the increase in CD3⁺ T cells in lung ELT observed in the original study (16), MIG (CXCL9) and ITAC (CXCL11) recruit and position activated T-cells (55). CCL chemokines can also recruit monocytes, dendritic cells, lymphocytes, and eosinophils, which collectively promote cSiO₂-induced inflammation and autoimmunity in pleiotropic manners (56–58).

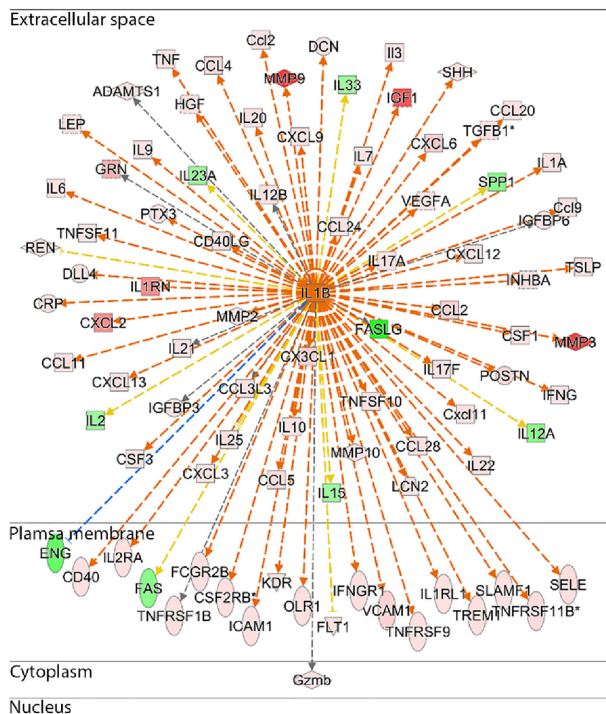
cSiO₂-triggered release of extracellular enzymes into the alveolar fluid and suppression of these responses by DHA also have significant implications to inflammation and autoimmunity in the lung. cSiO₂ induction of matrix metalloproteinases (MMPs), a family of enzymes that degrade extracellular matrix and basement membrane components, is consistent with prior *in vivo* and *in vitro* investigations (59). cSiO₂ also elicited extracellular granzyme B, which has been linked to lupus pathogenesis by cleaving autoantigens and exposing neoepitopes, as well as ACE and the aspartic acid protease renin 1, two key enzymes in the renin-angiotensin system. The latter regulates many physiological functions, including inflammation, and has been previously shown to play a role in silicosis in mice and rats (60–64).

Elevated soluble adhesion molecules in the BALF following cSiO₂ instillation are highly indicative of persistent inflammation, extracellular matrix breakdown, and potentially, as a means of negative feedback inhibition in the lung. Selectins have a key role in inflammation by mediating leukocyte rolling, adhesion, and transmigration into inflamed tissues. Leukocyte (L)-selectin (CD62L) is expressed on neutrophils, monocytes, and most lymphocytes (65) and is a biomarker of inflammation and autoimmune disease, and notably, occupational exposure to

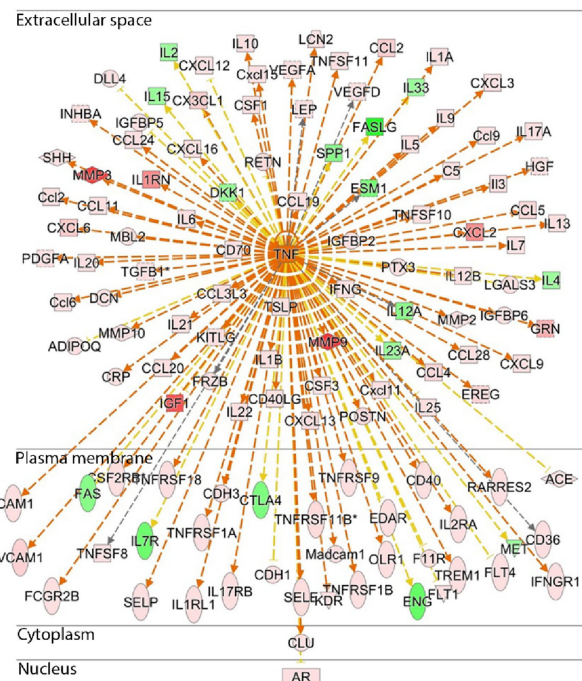
A

Upstream Regulator	Molecule Type	Predicted Activation State	Activation or Inhibition Z score	
			cSiO2	cSiO2 +DHA
TNF	Cytokine	Activated	6.197	5.564
IL-1β	Cytokine	Activated	6.591	6.015
IL-10	Cytokine	Inhibited	-1.868	-2.009
IL-6	Cytokine	Activated	4.361	4.375
IFNG	Cytokine	Activated	4.39	4.061
IL-17A	Cytokine	Activated	4.856	3.999
IL-4	Cytokine	Activated	3.219	2.668
NF-κB (complex)	Complex	Activated	5.41	4.955

B



C



Prediction Legend

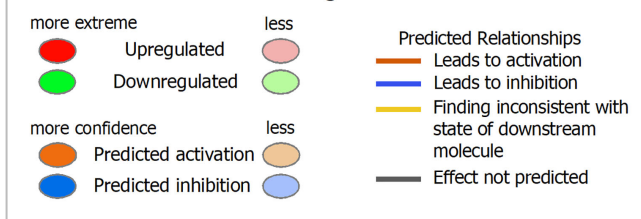
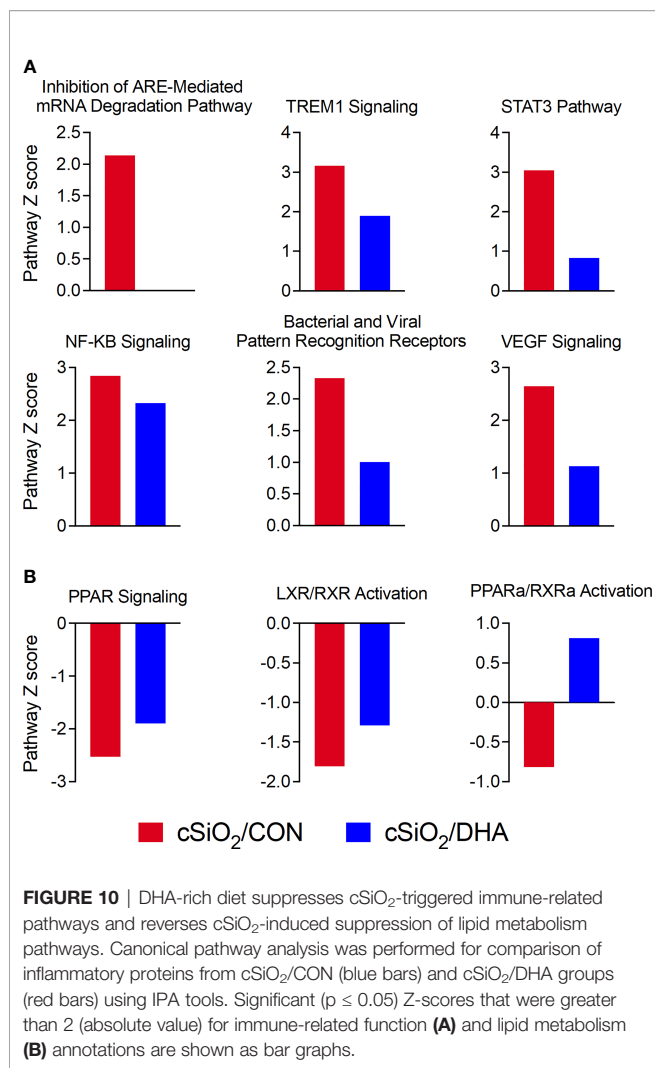


FIGURE 9 | DHA supplementation negatively influences major upstream regulators of cSiO₂-induced inflammatory protein expression. **(A)** Top upstream regulators present in cSiO₂/CON and cSiO₂/DHA treatments in BALF were predicted by IPA. Positive Z-score indicates activation, and negative Z-score indicates inhibition. Targets of **(B)** IL-1β and **(C)** TNF-α present in data set. Up-regulated and down-regulated proteins are highlighted in red and green, respectively, and the color depth is correlated to the fold change. Orange and blue dashed lines with arrows indicate indirect activation and inhibition, respectively. Yellow and gray dashed lines with arrows depict inconsistent effects and no prediction, respectively.



cSiO₂ (62–64). Endothelial (E)-selectin (CD62E) and platelet (P)-selectin are biomarkers in autoimmune and rheumatic diseases (66–69). DHA suppression of adhesion molecules in the alveolar fluid observed in this study is remarkably in agreement with the findings in plasma of prior preclinical and clinical investigations of ω -3 PUFAs (70).

Consistent with extracellular matrix breakdown, cSiO₂ induced release of soluble TNF superfamily members into the alveolar fluid, and their induction was suppressed by DHA consumption. The ligand-receptor pairs CD40L-CD40 and OX40L-OX40 represent critical immune checkpoints for B cell differentiation, antigen presenting cell activation, and T cell modulation (71). High serum levels sCD40L or sOX40L have been reported in lupus and other rheumatic autoimmune diseases (72, 73). CD6, a lymphocyte surface receptor that associates with the T cell receptor/CD3 complex, acts as a co-stimulatory molecule for T cell activation (74). sCD6 is detectable in patients with systemic autoimmune and inflammatory disorders (75, 76). Other TNF receptor superfamily proteins that were upregulated by cSiO₂,

downregulated by DHA, and have pertinence to lupus and autoimmunity include sBAFFR (77), sTNFR1 and sTNFR2 (43), and sTRAIL (78–80).

Strengths of this investigation include employment of a widely utilized lupus-prone mouse model, a well-recognized autoimmune trigger, and a human-relevant dose of DHA. However, this investigation had several limitations that require additional consideration in future studies. Since this was a discovery-based approach, we employed a single standard dilution for BALF and plasma and used MFI as a measure of protein signal, thus limiting our ability to perform absolute quantitation of inflammatory proteins identified herein. Nevertheless, proteins of further interest can be quantified by ELISA in future studies employing our preclinical model. Additionally, the dose of cSiO₂ employed here to induce autoimmunity in the NZBWF1 mouse represents one half of a human equivalent lifetime exposure to cSiO₂ at the recommended NIOSH exposure limit (15). The inability to adequately clear particles at this high dose likely unleashes a vicious cycle of inflammation, cell death, and re-release of cSiO₂. This propensity for unresolved inflammation appeared to overwhelm DHA's capacity to suppress induction of some inflammatory proteins by wk 13, suggesting there is a limit to its ameliorative action. Thus, additional insights could be gained by replicating this study using lower cSiO₂ doses and extending experiment duration.

A further limitation of this study is that since we did not include a non-autoimmune strain in our parent investigation, it could be argued that the observed protein signatures may be a generalized inflammatory response to cSiO₂ that happens to coincide with autoimmunity in this lupus-prone mouse strain. However, in an earlier prior study, we compared the effects to cSiO₂ and DHA in female NZBWF1 mice to those for one of the parental lines, female NZW/LacJ, which does not exhibit the propensity towards autoimmunity (81). At 12 wk PI, the NZBWF1 mice exhibited marked macrophage, neutrophil, and lymphocyte infiltration with robust ectopic lymphoid tissue neogenesis in the lung that were suppressed by DHA feeding. In comparison, inflammatory cell responses in the lung and kidney to cSiO₂ were extremely modest in the NZW/LacJ mice but were nonetheless ameliorated by DHA supplementation. Inflammatory and autoimmune responses to cSiO₂ are likewise much lower in female C57BL/6 mice, another mouse strain with low lupus predilection (15). Thus, it could be speculated that cSiO₂-induced inflammatory proteome would be similarly less robust in NZW/LacJ and C57BL/6 mice, however, this supposition will need future confirmation using these non-autoimmune strains and extending the study length beyond three months after cSiO₂ treatment.

In conclusion, the demonstration here that DHA prevents or delays cSiO₂-triggered inflammatory protein expression in NZBWF1 mice provides new insights pathways by which ω -3 PUFAs interfere with environmental triggering of chronic inflammation and autoimmune disease. These findings have resonance with one of the four goals of the 2020-2030 Strategic Plan for NIH Nutrition Research which is to develop precision nutrition strategies to reduce the burden of disease in clinical

settings (82). The DHA diet used here equates to human intake of 5 g/d, which is a realistic and safe human dose (83). Consistent with our findings, ameliorative effects on inflammatory mediators or inflammatory cell function in human investigations have been found at marine ω -3 PUFA intakes of > 2 g/d (21), and a recent meta-analysis of human clinical trials determined that supplementation with 3 g/d could benefit patients with lupus (33). Taken together, ω -3 supplementation could be a precision nutrition approach for delaying progression of autoimmunity and reducing lupus flaring following respiratory exposures to cSiO₂ or potentially other airborne particles.

DATA AVAILABILITY STATEMENT

Original proteomic datasets from this study are available in a publicly accessible repository: <https://doi.org/10.26078/W1G0-KB31>. Other existing gene and autoantibody expression datasets used in this study are available at <https://doi.org/10.26078/4697-1p77> and <https://datadryad.org/stash/share/LLav72h-OvhiPYfqma2-qzCSzeZCJIts55UWwaXqzA>, respectively.

ETHICS STATEMENT

The animal study was reviewed and approved by Institutional Animal Care and Use Committee at Michigan State University (AUF #01/15-021-00).

AUTHOR CONTRIBUTIONS

LR: data curation, data analysis/interpretation, figure preparation, manuscript writing. MB: study design, animal study, necropsy, immunohistochemical analyses and morphometry, manuscript preparation and manuscript editing. AB and KW: data analysis/interpretation, figure preparation, manuscript editing. JH: study design, lung/kidney histopathology, morphometry, data analyses. JP: study design, coordination, oversight, funding acquisition, manuscript preparation and submission. All authors contributed to the article and approved the submitted version.

FUNDING

This research was funded by NIH ES027353 (JP), NIH F31ES030593 (KW), NIH T32ES007255 (KW), Lupus Foundation of America (JP, KW), USDA National Institute of Food and Agriculture Hatch Projects 1020129 (JP) and UTA-01407 and UTA-01456 (AB), and the Dr.Robert and Carol Deibel Family Endowment (JP).

ACKNOWLEDGMENTS

The authors thank Dr. Andrij Holian and Dr. James Wagner for invaluable advice and assistance on conducting these experiments.

Thanks to Adrianna Kirby for assistance with the statistics and data visualization.

SUPPLEMENTARY MATERIAL

The Supplementary Material for this article can be found online at: <https://www.frontiersin.org/articles/10.3389/fimmu.2021.781446/full#supplementary-material>

Supplementary Figure 1 | cSiO₂-induced cytokines in BALF are modestly decreased by DHA supplementation. **(A)** Heat maps with unsupervised clustering (Euclidian distance method) depict unit variance-scaled mean fluorescent intensity for cytokines measured in the BALF. Blue, red and green in the top bar indicates the VEH/CON, cSiO₂/CON, and cSiO₂/DHA groups, respectively, at 1, 5, 9, or 13 wks PI. Scale bar values reflect the range of variance-stabilized mean fluorescent intensities (MFIs), which were centered across rows. **(B)** DHA diet suppresses cSiO₂-induced selected cytokines in BALF over time. MFIs were obtained using the microarray panel for VEH- or cSiO₂-exposed mice fed CON or DHA diets. Data for select proteins were analyzed by two-way ANOVA for main effects of timepoint and treatment with *post-hoc* Tukey HSD multiple comparison tests to determine effects of treatment at each time point. Data are mean \pm SEM. Main effect p-values for timepoint, treatment, and the interaction of these factors are shown below the plots. Symbols indicate significant differences ($p \leq 0.05$) as follows: * for cSiO₂/CON vs. VEH/CON; # for cSiO₂/DHA vs. VEH/CON; and + for cSiO₂/CON vs. cSiO₂/DHA.

Supplementary Figure 2 | cSiO₂-induced TNF superfamily proteins in BALF are suppressed by intake of DHA-rich diet. Heat maps with unsupervised clustering (Euclidian distance method) depict unit variance-scaled mean fluorescent intensity for TNF superfamily proteins expression measured in the BALF. Blue, red and green in the top bar indicates the VEH/CON, cSiO₂/CON, and cSiO₂/DHA groups, respectively, at 1, 5, 9, or 13 wks PI. Scale bar values reflect the range of variance-stabilized MFIs, which were centered across rows. **(B)** DHA diet suppresses selected cSiO₂-induced TNF superfamily proteins in BALF over time. Mean fluorescent intensities were obtained using the microarray panel for vehicle (VEH)- or cSiO₂-exposed mice fed CON or DHA diets. Data for select proteins were analyzed by two-way ANOVA for main effects of timepoint and treatment with *post-hoc* Tukey HSD multiple comparison tests to determine effects of treatment at each time point. Data are mean \pm SEM. Main effect p-values for timepoint, treatment, and the interaction of these factors are shown below the plots. Symbols indicate significant differences ($p \leq 0.05$) as follows: * for cSiO₂/CON vs. VEH/CON; # for cSiO₂/DHA vs. VEH/CON; and + for cSiO₂/CON vs. cSiO₂/DHA.

Supplementary Figure 3 | cSiO₂-induced signal transduction proteins expression in BALF are suppressed by intake of DHA rich diet. **(A)** Heat maps with unsupervised clustering (Euclidian distance method) depict unit variance-scaled mean fluorescent intensity for signal transduction proteins expression measured in the BALF. Blue, red and green in the top bar indicates the VEH/CON, cSiO₂/CON, and cSiO₂/DHA groups, respectively, at 1, 5, 9, or 13 wks PI. Scale bar values reflect the range of variance-stabilized mean fluorescent intensities (MFIs), which were centered across rows. **(B)** DHA diet suppresses cSiO₂-induced selected signal transduction proteins in BALF over time. MFIs were obtained using the microarray panel for vehicle (VEH)- or cSiO₂-exposed mice fed CON or DHA diets. Data for select proteins were analyzed by two-way ANOVA for main effects of timepoint and treatment with *post-hoc* Tukey HSD multiple comparison tests to determine effects of treatment at each time point. Data are mean \pm SEM. Main effect p-values for timepoint, treatment, and the interaction of these factors are shown below the plots. Symbols indicate significant differences ($p \leq 0.05$) as follows: * for cSiO₂/CON vs. VEH/CON; # for cSiO₂/DHA vs. VEH/CON; and + for cSiO₂/CON vs. cSiO₂/DHA.

Supplementary Figure 4 | Effects of DHA intake on cSiO₂-induced inflammatory protein responses in plasma. Heat maps with unsupervised clustering (Euclidian distance method) depict mean fluorescent intensities (MFIs) for 203 proteins. Black, red, and Blue in the top bar indicates the VEH/CON, cSiO₂/CON, and cSiO₂/DHA groups, respectively, at 1, 5, 9, or 13 wks PI. Scale bar values reflect the

range of variance-stabilized mean fluorescent intensities, which were centered across rows.

Supplementary Figure 5 | Effects of DHA on cSiO₂-induced chemokine expression in BALF and plasma are similar. **(A)** Summary of proteins altered in cSiO₂/CON and cSiO₂/DHA mice in BALF over time. DHA supplementation suppresses cSiO₂-induced chemokine expression in plasma **(B)** and BALF **(C)** over time. Z-score for chemokine proteins was calculated using mean fluorescent intensities of chemokine proteins belonging to chemokine category **(Supplemental Table 1)**. Missing values and outliers were handled as described in the Methods section. Data for select proteins were analyzed by two-way ANOVA for main effects of timepoint and treatment with *post-hoc* Tukey HSD

multiple comparison tests to determine effects of treatment at each time point. Data are mean ± SEM. Main effect p-values for timepoint, treatment, and the interaction of these factors are shown below the plots. Symbols indicate significant differences ($p \leq 0.05$) as follows: * for cSiO₂/CON vs. VEH/CON; # for cSiO₂/DHA vs. VEH/CON; and + for cSiO₂/CON vs. cSiO₂/DHA. **(D)** BALF chemokine protein responses positively correlate with corresponding plasma chemokine protein responses. Scatter plots for Z scores from chemokines in plasma vs. Z scores from chemokine in BALF in each animal. Linear regression lines with 95% confidence intervals (curved lines) are shown along with the Spearman ρ value and p-value. **(E)** Correlation between selected individual chemokines in BALF and same chemokine in plasma for individual animals was assessed by Spearman's correlation coefficient at wk 9. * $p < 0.05$.

REFERENCES

- Pons-Estel GJ, Ugarte-Gil MF, Alarcon GS. Epidemiology of Systemic Lupus Erythematosus. *Expert Rev Clin Immunol* (2017) 13(8):799–814. doi: 10.1080/1744666X.2017.1327352
- Flores-Mendoza G, Sanson SP, Rodriguez-Castro S, Crispin JC, Rosetti F. Mechanisms of Tissue Injury in Lupus Nephritis. *Trends Mol Med* (2018) 4(4):364–78. doi: 10.1016/j.molmed.2018.02.003
- Moulton VR, Suarez-Fueyo A, Meidan E, Li H, Mizui M, Tsokos GC. Pathogenesis of Human Systemic Lupus Erythematosus: A Cellular Perspective. *Trends Mol Med* (2017) 23(7):615–35. doi: 10.1016/j.molmed.2017.05.006
- Basta F, Fasola F, Triantafyllidis K, Schwarting A. Systemic Lupus Erythematosus (SLE) Therapy: The Old and the New. *Rheumatol Ther* (2020) 7(3):433–46. doi: 10.1007/s40744-020-00212-9
- Parks CG, de Souza Espindola Santos A, Barbhaya M, Costenbader KH. Understanding the Role of Environmental Factors in the Development of Systemic Lupus Erythematosus. *Best Pract Res Clin Rheumatol* (2017) 31(3):306–20. doi: 10.1016/j.berh.2017.09.005
- Barnes H, Goh NSL, Leong TL, Hoy R. Silica-Associated Lung Disease: An Old-World Exposure in Modern Industries. *Respirology* (2019) 24(12):1165–75. doi: 10.1111/resp.13695
- Parks CG, Cooper GS, Nylander-French LA, Sanderson WT, Dement JM, Cohen PL, et al. Occupational Exposure to Crystalline Silica and Risk of Systemic Lupus Erythematosus: A Population-Based, Case-Control Study in the Southeastern United States. *Arthritis Rheum* (2002) 46(7):1840–50. doi: 10.1002/art.10368
- Pollard KM. Silica, Silicosis, and Autoimmunity. *Front Immunol* (2016) 7:97. doi: 10.3389/fimmu.2016.00097
- Morotti A, Sollaku I, Catalani S, Franceschini F, Cavazzana I, Fredi M, et al. Systematic Review and Meta-Analysis of Epidemiological Studies on the Association of Occupational Exposure to Free Crystalline Silica and Systemic Lupus Erythematosus. *Rheumatol* (2021) 60(1):81–91. doi: 10.1093/rheumatology/keaa444
- Brown J, Archer A, Pfau J, Holian A. Silica Accelerated Systemic Autoimmune Disease in Lupus-Prone New Zealand Mixed Mice. *Clin Exp Immunol* (2003) 131(3):415–21. doi: 10.1046/j.1365-2249.2003.02094.x
- Brown JM, Pfau JC, Holian A. Immunoglobulin and Lymphocyte Responses Following Silica Exposure in New Zealand Mixed Mice. *Inhal Toxicol* (2004) 16(3):133–9. doi: 10.1080/08958370490270936
- Brown JM, Pfau JC, Pershouse MA, Holian A. Silica, Apoptosis, and Autoimmunity. *J Immunotoxicol* (2005) 1(3):177–87. doi: 10.1080/15476910490911922
- Clark A, Zhao EJ, Birukova A, Buckley ES, Ord JR, Asfaw YG, et al. Inhaled Silica Induces Autoimmunity in a Strain-Dependent Manner. *J Immunol* (2017) 198(1 Supplement):58.13–3.
- Foster MH, Ord JR, Zhao EJ, Birukova A, Fee L, Korte FM, et al. Silica Exposure Differentially Modulates Autoimmunity in Lupus Strains and Autoantibody Transgenic Mice. *Front Immunol* (2019) 10:2336. doi: 10.3389/fimmu.2019.02336
- Bates MA, Brandenberger C, Langohr I, Kumagai K, Harkema JR, Holian A, et al. Silica Triggers Inflammation and Ectopic Lymphoid Neogenesis in the Lungs in Parallel With Accelerated Onset of Systemic Autoimmunity and Glomerulonephritis in the Lupus-Prone NZBWF1 Mouse. *PLoS One* (2015) 10(5):e0125481. doi: 10.1371/journal.pone.0125481
- Bates M, Akbari P, Gilley K, Jackson-Humbles D, Wagner J, Li N, et al. Dietary Docosahexaenoic Acid Prevents Silica-Induced Development of Pulmonary Ectopic Germinal Centers and Glomerulonephritis in the Lupus-Prone NZBWF1 Mouse. *Front Immunol* (2018) 9:2002. doi: 10.3389/fimmu.2018.02002
- Pollard KM, Cauvi DM, Mayeux JM, Toomey CB, Peiss AK, Hultman P, et al. Mechanisms of Environment-Induced Autoimmunity. *Annu Rev Pharmacol Toxicol* (2021) 61:135–57. doi: 10.1146/annurev-pharmtox-031320-111453
- Calder PC. Omega-3 Fatty Acids and Inflammatory Processes: From Molecules to Man. *Biochem Soc Trans* (2017) 45(5):1105–15. doi: 10.1042/BST20160474
- Harris WS, Tintle NL, Imamura F, Qian F, Korat AVA, Marklund M, et al. Blood N-3 Fatty Acid Levels and Total and Cause-Specific Mortality From 17 Prospective Studies. *Nat Commun* (2021) 12(1):2329. doi: 10.1038/s41467-021-22370-2
- Ferreira HB, Pereira AM, Melo T, Paiva A, Domingues MR. Lipidomics in Autoimmune Diseases With Main Focus on Systemic Lupus Erythematosus. *J Pharm BioMed Anal* (2019) 174:386–95. doi: 10.1016/j.jpba.2019.06.005
- Akbar U, Yang M, Kurian D, Mohan C. Omega-3 Fatty Acids in Rheumatic Diseases: A Critical Review. *J Clin Rheumatol* (2017) 23(6):330–9. doi: 10.1097/rhu.0000000000000563
- Lands B, Bibus D, Stark KD. Dynamic Interactions of N-3 and N-6 Fatty Acid Nutrients. *Prostaglandins Leukotrienes Essential Fatty Acids (PLEFA)* (2018) 136:15–21. doi: 10.1016/j.plefa.2017.01.012
- Harris WS, Tintle NL, Etherton MR, Vasani RS. Erythrocyte Long-Chain Omega-3 Fatty Acid Levels Are Inversely Associated With Mortality and With Incident Cardiovascular Disease: The Framingham Heart Study. *J Clin Lipidol* (2018) 12(3):718–27.e6. doi: 10.1016/j.jacl.2018.02.010
- Robinson DR, Prickett JD, Makoul GT, Steinberg AD, Colvin RB. Dietary Fish Oil Reduces Progression of Established Renal Disease in (NZB X NZW)F1 Mice and Delays Renal Disease in BXSb and MRL/1 Strains. *Arthritis Rheum* (1986) 29(4):539–46. doi: 10.1002/art.1780290412
- Robinson DR, Xu LL, Knoell CT, Tateno S, Olesiak W. Modification of Spleen Phospholipid Fatty Acid Composition by Dietary Fish Oil and by N-3 Fatty Acid Ethyl Esters. *J Lipid Res* (1993) 34(8):1423–34. doi: 10.1016/S0022-2275(20)36971-6
- Lim BO, Jolly CA, Zaman K, Fernandes G. Dietary (N-6) and (N-3) Fatty Acids and Energy Restriction Modulate Mesenteric Lymph Node Lymphocyte Function in Autoimmune-Prone (NZB X NZW)F1 Mice. *J Nutr* (2000) 130(7):1657–64. doi: 10.1093/jn/130.7.1657
- Jolly CA, Muthukumar A, Avula CP, Troyer D, Fernandes G. Life Span is Prolonged in Food-Restricted Autoimmune-Prone (NZB X NZW)F1 Mice Fed a Diet Enriched With (N-3) Fatty Acids. *J Nutr* (2001) 131(10):2753–60. doi: 10.1093/jn/131.10.2753
- Bhattacharya A, Lawrence RA, Krishnan A, Zaman K, Sun D, Fernandes G. Effect of Dietary N-3 and N-6 Oils With and Without Food Restriction on Activity of Antioxidant Enzymes and Lipid Peroxidation in Livers of Cyclophosphamide Treated Autoimmune-Prone NZB/W Female Mice. *J Am Coll Nutr* (2003) 22(5):388–99. doi: 10.1080/07315724.2003.10719322
- Halade GV, Rahman MM, Bhattacharya A, Barnes JL, Chandrasekar B, Fernandes G. Docosahexaenoic Acid-Enriched Fish Oil Attenuates Kidney Disease and Prolongs Median and Maximal Life Span of Autoimmune Lupus-Prone Mice. *J Immunol* (2010) 184(9):5280–6. doi: 10.4049/jimmunol.0903282

30. Halade GV, Williams PJ, Veigas JM, Barnes JL, Fernandes G. Concentrated Fish Oil (Lovaza (R)) Extends Lifespan and Attenuates Kidney Disease in Lupus-Prone Short-Lived (NZBxNZW)F1 Mice. *Exp Bio Med* (2013) 238 (6):610–22. doi: 10.1177/1535370213489485
31. Pestka JJ, Vines LL, Bates MA, He K, Langohr I. Comparative Effects of N-3, N-6 and N-9 Unsaturated Fatty Acid-Rich Diet Consumption on Lupus Nephritis, Autoantibody Production and CD4+ T Cell-Related Gene Responses in the Autoimmune NZBWF1 Mouse. *PLoS One* (2014) 9(6): e100255. doi: 10.1371/journal.pone.0100255
32. Li X, Bi X, Wang S, Zhang Z, Li F, Zhao AZ. Therapeutic Potential of ω -3 Polyunsaturated Fatty Acids in Human Autoimmune Diseases. *Front Immunol* (2019) 10:2241. doi: 10.3389/fimmu.2019.02241
33. Duarte-García A, Myasoedova E, Karmacharya P, Hocaoglu M, Murad MH, Warrington KJ, et al. Effect of Omega-3 Fatty Acids on Systemic Lupus Erythematosus Disease Activity: A Systematic Review and Meta-Analysis. *Autoimmun Rev* (2020) 19(12):102688. doi: 10.1016/j.autrev.2020.102688
34. Charoenwoodhipong P, Harlow SD, Marder W, Hassett AL, McCune WJ, Gordon C, et al. Dietary Omega Polyunsaturated Fatty Acid Intake and Patient-Reported Outcomes in Systemic Lupus Erythematosus: The Michigan Lupus Epidemiology & Surveillance (MILES) Program. *Arthr Care Res* (2019) 72(7):874–81. doi: 10.1002/acr.23925
35. Benninghoff AD, Bates MA, Chauhan PS, Wierenga KA, Gilley KN, Holian A, et al. Docosahexaenoic Acid Consumption Impedes Early Interferon- and Chemokine-Related Gene Expression While Suppressing Silica-Triggered Flaring of Murine Lupus. *Front Immunol* (2019) 10:2851(2851). doi: 10.3389/fimmu.2019.02851
36. Rajasinghe LD, Li Q-Z, Zhu C, Yan M, Chauhan PS, Wierenga KA, et al. Omega-3 Fatty Acid Intake Suppresses Induction of Diverse Autoantibody Repertoire by Crystalline Silica in Lupus-Prone Mice. *Autoimmunity* (2020) 10.1080/08916934.2020.1801651:1–19. doi: 10.1080/08916934.2020.1801651
37. Metsalu T, Vilo J. ClustVis: A Web Tool for Visualizing Clustering of Multivariate Data Using Principal Component Analysis and Heatmap. *Nucleic Acids Res* (2015) 43(W1):W566–W70. doi: 10.1093/nar/gkv468
38. Wierenga KA, Harkema JR, Pestka JJ. Lupus, Silica, and Dietary Omega-3 Fatty Acid Interventions. *Toxicol Pathol* (2019) 47(8):1004–11. doi: 10.1177/0192623319878398
39. Kawasaki H. A Mechanistic Review of Silica-Induced Inhalation Toxicity. *Inhal Toxicol* (2015) 27(8):363–77. doi: 10.3109/08958378.2015.1066905
40. Herseth J, Refsnes M, Låg M, Hetland G, Schwarze P. IL-1beta as a Determinant in Silica-Induced Cytokine Responses in Monocyte-Endothelial Cell Co-Cultures. *Hum Exp Toxicol* (2008) 27(5):387–99. doi: 10.1177/0960327108094610
41. Chauhan PS, Wagner JG, Benninghoff AD, Lewandowski RP, Favor OK, Wierenga KA, et al. Rapid Induction of Pulmonary Inflammation, Autoimmune Gene Expression, and Ectopic Lymphoid Neogenesis Following Acute Silica Exposure in Lupus-Prone Mice. *Front Immunol* (2021) 12:635138. doi: 10.3389/fimmu.2021.635138
42. Grytting VS, Refsnes M, Øvrevik J, Halle MS, Schönenberger J, van der Lelij R, et al. Respirable Stone Particles Differ in Their Ability to Induce Cytotoxicity and Pro-Inflammatory Responses in Cell Models of the Human Airways. *Part Fibre Toxicol* (2021) 18(1):18. doi: 10.1186/s12989-021-00409-y
43. Skuland T, Lag M, Gutleb AC, Brinchmann BC, Serchi T, Ovrevik J, et al. Pro-Inflammatory Effects of Crystalline- and Nano-Sized Non-Crystalline Silica Particles in a 3D Alveolar Model. *Part Fibre Toxicol* (2020) 17(1):13. doi: 10.1186/s12989-020-00345-3
44. Svetič A, Finkelman FD, Jian YC, Dieffenbach CW, Scott DE, McCarthy KF, et al. Cytokine Gene Expression After *In Vivo* Primary Immunization With Goat Antibody to Mouse IgD Antibody. *J Immunol* (1991) 147(7):2391–7.
45. Wong SW, Kwon MJ, Choi AM, Kim HP, Nakahira K, Hwang DH. Fatty Acids Modulate Toll-Like Receptor 4 Activation Through Regulation of Receptor Dimerization and Recruitment Into Lipid Rafts in a Reactive Oxygen Species-Dependent Manner. *J Biol Chem* (2009) 284(40):27384–92. doi: 10.1074/jbc.M109.044065
46. Norris PC, Dennis EA. Omega-3 Fatty Acids Cause Dramatic Changes in TLR4 and Purinergic Eicosanoid Signaling. *Proc Natl Acad Sci USA* (2012) 109(22):8517–22. doi: 10.1073/pnas.1200189109
47. Norris PC, Gosselin D, Reichart D, Glass CK, Dennis EA. Phospholipase A2 Regulates Eicosanoid Class Switching During Inflammation Activation. *Proc Natl Acad Sci USA* (2014) 111(35):12746–51. doi: 10.1073/pnas.1404372111
48. Li X, Yu Y, Funk CD. Cyclooxygenase-2 Induction in Macrophages Is Modulated by Docosahexaenoic Acid via Interactions With Free Fatty Acid Receptor 4 (FFA4). *FASEB J* (2013) 27(12):4987–97. doi: 10.1096/fj.13-235333
49. Yan Y, Jiang W, Spinetti T, Tardivel A, Castillo R, Bourquin C, et al. Omega-3 Fatty Acids Prevent Inflammation and Metabolic Disorder Through Inhibition of NLRP3 Inflammasome Activation. *Immunity* (2013) 38 (6):1154–63. doi: 10.1016/j.immuni.2013.05.015
50. Ricote M, Glass CK. PPARs and Molecular Mechanisms of Transrepression. *Biochim Biophys Acta* (2007) 1771(8):926–35. doi: 10.1016/j.bbali.2007.02.013
51. Chang HY, Lee H-N, Kim W, Surh Y-J. Docosahexaenoic Acid Induces M2 Macrophage Polarization Through Peroxisome Proliferator-Activated Receptor γ Activation. *Life Sci* (2015) 120:39–47. doi: 10.1016/j.lfs.2014.10.014
52. Christie WW, Harwood JL. Oxidation of Polyunsaturated Fatty Acids to Produce Lipid Mediators. *Essays Biochem* (2020) 64(3):401–21. doi: 10.1042/ebc20190082
53. Duvall MG, Levy BD. DHA- and EPA-Derived Resolvins, Protectins, and Maresins in Airway Inflammation. *Eur J Pharmacol* (2016) 785:144–55. doi: 10.1016/j.ejphar.2015.11.001
54. Kruger P, Saffarzadeh M, Weber AN, Rieber N, Radsak M, von Bernuth H, et al. Neutrophils: Between Host Defence, Immune Modulation, and Tissue Injury. *PLoS Pathog* (2015) 11(3):e1004651. doi: 10.1371/journal.ppat.1004651
55. Karin N. CXCR3 Ligands in Cancer and Autoimmunity, Chemoattraction of Effector T Cells, and Beyond. *Front Immunol* (2020) 11:976. doi: 10.3389/fimmu.2020.00976
56. Qidwai T. Chemokine Genetic Polymorphism in Human Health and Disease. *Immunol Lett* (2016) 176:128–38. doi: 10.1016/j.imlet.2016.05.018
57. Sarafi MN, Garcia-Zepeda EA, MacLean JA, Charo IF, Luster AD. Murine Monocyte Chemoattractant Protein (MCP)-5: A Novel CC Chemokine That Is a Structural and Functional Homologue of Human MCP-1. *J Exp Med* (1997) 185(1):99–109. doi: 10.1084/jem.185.1.99
58. Scapini P, Laudanna C, Pinardi C, Allavena P, Mantovani A, Sozzani S, et al. Neutrophils Produce Biologically Active Macrophage Inflammatory Protein-3alpha (MIP-3alpha)/CCL20 and MIP-3beta/CCL19. *Eur J Immunol* (2001) 31 (7):1981–8. doi: 10.1002/1521-4141(200107)31:7<1981::aid-immu1981>3.0.co;2-x
59. Liu J, Khalil RA. Matrix Metalloproteinase Inhibitors as Investigational and Therapeutic Tools in Unrestrained Tissue Remodeling and Pathological Disorders. *Prog Mol Biol Transl Sci* (2017) 148:355–420. doi: 10.1016/bs.pmbts.2017.04.003
60. Russell AI, Cunninghame Graham DS, Chadha S, Robertson C, Fernandez-Hart T, Griffiths B, et al. No Association Between E- and L-Selectin Genes and SLE: Soluble L-Selectin Levels do Correlate With Genotype and a Subset in SLE. *Genes Immun* (2005) 6(5):422–9. doi: 10.1038/sj.gene.6364222
61. Patel M, Oni L, Midgley A, Smith E, Tullus K, Marks SD, et al. Increased Concentration of Plasma TNFR1 and TNFR2 in Paediatric Lupus Nephritis. *Lupus* (2016) 25(9):1040–4. doi: 10.1177/09612033166631634
62. Li S, Li Y, Zhang Y, Li S, Zhang M, Jin F, et al. Yang F. N-Acetyl-Seryl-Aspartyl-Lysyl-Proline Regulates Lung Renin Angiotensin System to Inhibit Epithelial-Mesenchymal Transition in Silicotic Mice. *Toxicol Appl Pharmacol* (2020) 408:115255. doi: 10.1016/j.taap.2020.115255
63. Gao X, Xu H, Zhang B, Tao T, Liu Y, Xu D, et al. Interaction of N-Acetyl-Seryl-Aspartyl-Lysyl-Proline With the Angiotensin-Converting Enzyme 2-Angiotensin-(1-7)-Mas Axis Attenuates Pulmonary Fibrosis in Silicotic Rats. *Exp Physiol* (2019) 104(10):1562–74. doi: 10.1113/ep087515
64. Zhang BN, Zhang X, Xu H, Gao XM, Zhang GZ, Zhang H, et al. Dynamic Variation of RAS on Silicotic Fibrosis Pathogenesis in Rats. *Curr Med Sci* (2019) 39(4):551–9. doi: 10.1007/s11596-019-2073-8
65. Ivetic A, Hoskins Green HL, Hart SJ. L-Selectin: A Major Regulator of Leukocyte Adhesion, Migration and Signaling. *Front Immunol* (2019) 10:1068(1068). doi: 10.3389/fimmu.2019.01068
66. Sfrikakis PP, Charalambopoulos D, Vaiopoulos G, Mavrikakis M. Circulating P- and L-Selectin and T-Lymphocyte Activation and Patients With Autoimmune Rheumatic Diseases. *Clin Rheumatol* (1999) 18(1):28–32. doi: 10.1007/s100670050047
67. Kuryliszyn-Moskal A, Klimiuk PA, Sierakowski S. Soluble Adhesion Molecules (sVCAM-1, sE-Selectin), Vascular Endothelial Growth Factor (VEGF) and Endothelin-1 in Patients With Systemic Sclerosis: Relationship to Organ Systemic Involvement. *Clin Rheumatol* (2005) 24(2):111–6. doi: 10.1007/s10067-004-0987-3

68. Nakatani K, Yoshimoto S, Asai O, Sakan H, Terada M, Saito Y, et al. Enhanced Expression of the Soluble Form of E-Selectin Attenuates Progression of Lupus Nephritis and Vasculitis in MRL/lpr Mice. *Immun Inflammation Dis* (2013) 1(1):37–46. doi: 10.1002/iid3.6
69. Nyberg F, Stephansson E. Elevated Soluble E-Selectin in Cutaneous Lupus Erythematosus. *Adv Exp Med Biol* (1999) 455:153–9. doi: 10.1007/978-1-4615-4857-7_22
70. Baker EJ, Yusof MH, Yaqoob P, Miles EA, Calder PC. Omega-3 Fatty Acids and Leukocyte-Endothelium Adhesion: Novel Anti-Atherosclerotic Actions. *Mol Aspects Med* (2018) 64:169–81. doi: 10.1016/j.mam.2018.08.002
71. Bellan M, Quaglia M, Nerviani A, Mauro D, Lewis M, Goegan F, et al. Increased Plasma Levels of Gas6 and Its Soluble Tyrosine Kinase Receptors Mer and Axl Are Associated With Immunological Activity and Severity of Lupus Nephritis. *Clin Exp Rheumatol* (2021) 39(1):132–8.
72. Goules A, Tzioufas AG, Manousakis MN, Kirou KA, Crow MK, Routsias JG. Elevated Levels of Soluble CD40 Ligand (Scd40l) in Serum of Patients With Systemic Autoimmune Diseases. *J Autoimmun* (2006) 26(3):165–71. doi: 10.1016/j.jaut.2006.02.002
73. An J, Ding S, Li S, Sun L, Chang X, Huang Z, et al. Enhancement of the Soluble Form of OX40 and OX40L Costimulatory Molecules But Reduction of the Membrane Form in Type 1 Diabetes (T1D). *J Immunol Res* (2019) 2019:1780567. doi: 10.1155/2019/1780567
74. Simões IT, Aranda F, Casadó-Llombart S, Velasco-de Andrés M, Català C, Álvarez P, et al. Multifaceted Effects of Soluble Human CD6 in Experimental Cancer Models. *J Immunother Cancer* (2020) 8(1):e000172. doi: 10.1136/jitc-2019-000172
75. Carrasco E, Escoda-Ferran C, Climent N, Miró-Julà C, Simões IT, Martínez-Florensa M, et al. Human Cd6 Down-Modulation Following T-Cell Activation Compromises Lymphocyte Survival and Proliferative Responses. *Front Immunol* (2017) 8:769. doi: 10.3389/fimmu.2017.00769
76. Ramos-Casals M, Font J, García-Carrasco M, Calvo J, Places L, Padilla O, et al. High Circulating Levels of Soluble Scavenger Receptors (Scd5 and Scd6) in Patients With Primary Sjögren's Syndrome. *Rheumatol* (2001) 40(9):1056–9. doi: 10.1093/rheumatology/40.9.1056
77. Silva M, Videira PA, Sackstein R. E-Selectin Ligands in the Human Mononuclear Phagocyte System: Implications for Infection, Inflammation, and Immunotherapy. *Front Immunol* (2018) 8:1878(1878). doi: 10.3389/fimmu.2017.01878
78. Liphaut BL, Kiss MHB, Carrasco S, Palmeira P, Goldenstein-Schainberg C, Carneiro-Sampaio M. Increased Serum Sfas, sTRAIL, and Reduced Sfasl in Juvenile-Onset Systemic Lupus Erythematosus. *Clin Rheumatol* (2017) 36(12):2847–52. doi: 10.1007/s10067-017-3615-8
79. Lub-de Hooge MN, de Vries EG, de Jong S, Bijl M. Soluble TRAIL Concentrations Are Raised in Patients With Systemic Lupus Erythematosus. *Ann Rheum Dis* (2005) 64(6):854–8. doi: 10.1136/ard.2004.029058
80. Saeed AM, Mogahed MM. Systemic Lupus Erythematosus Is Associated With Disturbed Cytokine Milieu and Increased Tnf-Related Apoptosis-Induced Ligand Levels. *Egypt J Immunol* (2016) 23(2):75–85.
81. Bates MA, Brandenberger C, Langohr II, Kumagai K, Lock AL, Harkema JR, et al. Silica-Triggered Autoimmunity in Lupus-Prone Mice Blocked by Docosahexaenoic Acid Consumption. *PLoS One* (2016) 11(8):e0160622. doi: 10.1371/journal.pone.0160622
82. Rodgers GP, Collins FS. Precision Nutrition—the Answer to “What to Eat to Stay Healthy”. *JAMA* (2020) 324(8):735–6. doi: 10.1001/jama.2020.13601
83. EFSA Panel on Dietetic Products N. Allergies. Scientific Opinion on the Extension of Use for DHA and EPA-Rich Algal Oil From *Schizochytrium* Sp. As a Novel Food Ingredient. *EFSA J* (2014) 12(10):3843. doi: 10.2903/j.efsa.2014.3843

Conflict of Interest: The authors declare that the research was conducted in the absence of any commercial or financial relationships that could be construed as a potential conflict of interest.

Publisher's Note: All claims expressed in this article are solely those of the authors and do not necessarily represent those of their affiliated organizations, or those of the publisher, the editors and the reviewers. Any product that may be evaluated in this article, or claim that may be made by its manufacturer, is not guaranteed or endorsed by the publisher.

Copyright © 2022 Rajasinghe, Bates, Benninghoff, Wierenga, Harkema and Pestka. This is an open-access article distributed under the terms of the Creative Commons Attribution License (CC BY). The use, distribution or reproduction in other forums is permitted, provided the original author(s) and the copyright owner(s) are credited and that the original publication in this journal is cited, in accordance with accepted academic practice. No use, distribution or reproduction is permitted which does not comply with these terms.